Tateno, C., Yoshizane, Y., Saito, N., Kataoka, M., Utoh, R., Yamasaki, C., Tachibana, A., Soeno, Y., Asahina, K. & other authors (2004). Near completely humanized liver in mice shows human-type metabolic responses to drugs. *Am J Pathol* **165**, 901–912.

Tsuge, M., Hiraga, N., Takaishi, H., Noguchi, C., Oga, H., Imamura, M., Takahashi, S., Iwao, E., Fujimoto, Y. & other authors (2005). Infection of human hepatocyte chimeric mouse with genetically engineered hepatitis B virus. *Hepatology* **42**, 1046–1054.

Vanwolleghem, T., Meuleman, P., Libbrecht, L., Roskams, T., De Vos, R. & Leroux-Roels, G. (2007). Ultra-rapid cardiotoxicity of the hepatitis C virus protease inhibitor BILN 2061 in the urokinase-type plasminogen activator mouse. *Gastroenterology* **133**, 1144–1155.

Vona, G., Tuveri, R., Delpuech, O., Vallet, A., Canioni, D., Ballardini, G., Trabut, J. B., Le Bail, B., Nalpas, B. & other authors (2004). Intrahepatic hepatitis C virus RNA quantification in microdissected hepatocytes. *J Hepatol* **40**, 682–688.

Wasley, A. & Alter, M. J. (2000). Epidemiology of hepatitis C: geographic differences and temporal trends. *Semin Liver Dis* **20**, 1–16.

Journal of General Virology (2010), 91, 1854–1864 DOI 10.1099/vir.0.019224-0

HBx protein is indispensable for development of viraemia in human hepatocyte chimeric mice

Masataka Tsuge,[1,2,3] Nobuhiko Hiraga,[1,3] Rie Akiyama,[1,3] Sachi Tanaka,[1,3] Miyuki Matsushita,[1,3] Fukiko Mitsui,[1,3] Hiromi Abe,[1,4] Shosuke Kitamura,[1,3] Tsuyoshi Hatakeyama,[1,3] Takashi Kimura,[1,3] Daiki Miki,[1,3] Nami Mori,[1,3] Michio Imamura,[1,3] Shoichi Takahashi,[1,3] C. Nelson Hayes[1,3] and Kazuaki Chayama[1,3,4]

Correspondence
Kazuaki Chayama
chayama@hiroshima-u.ac.jp

[1]Department of Medicine and Molecular Science, Division of Frontier Medical Science, Programs for Biomedical Research, Graduate School of Biomedical Sciences, Hiroshima University, Hiroshima, Japan

[2]Natural Science Center for Basic Research and Development, Hiroshima University, Hiroshima, Japan

[3]Liver Research Project Center, Hiroshima University, Hiroshima, Japan

[4]Laboratory for Liver Diseases, SNP Research Center, The Institute of Physical and Chemical Research (RIKEN), Yokohama, Japan

The non-structural X protein, HBx, of hepatitis B virus (HBV) is assumed to play an important role in HBV replication. Woodchuck hepatitis virus X protein is indispensable for virus replication, but the duck hepatitis B virus X protein is not. In this study, we investigated whether the HBx protein is indispensable for HBV replication *in vivo* using human hepatocyte chimeric mice. HBx-deficient (HBx-def) HBV was generated in HepG2 cells by transfection with an overlength HBV genome. Human hepatocyte chimeric mice were infected with HBx-def HBV with or without hepatic HBx expression by hydrodynamic injection of HBx expression plasmids. Serum virus levels and HBV sequences were determined with mice sera. The generated HBx-def HBV peaked in the sucrose density gradient at points equivalent to the generated HBV wild type and the virus in a patient's serum. HBx-def HBV-injected mice developed measurable viraemia only in continuously HBx-expressed liver. HBV DNA in the mouse serum increased up to 9 $\log_{10}$ copies ml^{-1} and the viraemia persisted for more than 2 months. Strikingly, all revertant viruses had nucleotide substitutions that enabled the virus to produce the HBx protein. It was concluded that the HBx protein is indispensable for HBV replication and could be a target for antiviral therapy.

Received 15 December 2009
Accepted 5 March 2010

INTRODUCTION

Chronic hepatitis B virus (HBV) infection is associated with the development of virus-related liver diseases, including chronic hepatitis, liver cirrhosis and hepatocellular carcinoma (HCC). HBV is a member of the family *Hepadnaviridae*, which consists of hepatotropic, small DNA viruses that infect their respective animal hosts (Ando *et al.*, 1999; Ganem & Schneider, 2001; Raney & McLachlan, 1991). HBV particles contain a 3.2 kb partially double-stranded circular DNA genome encoding four open reading frames (ORFs). The preS/S, pre-core/core, polymerase/reverse transcriptase and non-structural X protein (HBx) mRNAs are transcribed from each of the four ORFs (Seeger & Mason, 2000; Tang *et al.*, 2001). Although previous works have demonstrated that HBx protein is necessary for maximal HBV replication in cultured cells (Bouchard *et al.*, 2001; Keasler *et al.*, 2007; Leupin *et al.*, 2005; Tang *et al.*, 2005) and in mouse hepatocytes (Keasler *et al.*, 2007), the precise function of HBx in the virus life cycle remains poorly defined in human hepatocytes under physiological conditions because there is no natural infection–replication system available. Accordingly, all previous work has been done using hepatocarcinoma cell lines with transfection or mouse hepatocytes with hydrodynamic injection. Analysis of HBx under physiological conditions will provide more accurate information for the function of the HBx protein.

The nucleotide and amino acid sequences of the X genes are well-conserved among all mammalian hepadnaviruses. Expression of HBx protein in hepatocytes has been reported

The GenBank/EMBL/DDBJ accession number for the nucleotide sequence of the HBV genome cloned into plasmid pTRE-HB-wt is AB206817.

both in humans (Su *et al.*, 1998) and in woodchucks (Dandri *et al.*, 1996; Jacob *et al.*, 1997). Previous reports have shown that the X protein of the woodchuck hepatitis virus (WHV) is important for the virus life cycle (Chen *et al.*, 1993; Sitterlin *et al.*, 2000a; Zhang *et al.*, 2001; Zoulim *et al.*, 1994). In contrast, in non-oncogenic avian hepatitis viruses, such as duck hepatitis B virus (DHBV), the X protein (DHBx) is not necessary for virus replication *in vivo* (Meier *et al.*, 2003). The HBx and WHV X proteins (WHx) localize both in the cytoplasm and in the nucleus (Dandri *et al.*, 1998; Doria *et al.*, 1995; Sitterlin *et al.*, 2000b; Wang *et al.*, 1991), and both of them have similar multi-phasic activities for transcription, DNA repair, cell growth and apoptotic cell death in tissue-culture cells (Arbuthnot *et al.*, 2000; Murakami, 2001). HBx and WHx have also been shown to stimulate virus replication in cell lines by activating viral transcription (Colgrove *et al.*, 1989; Melegari *et al.*, 2005; Zhang *et al.*, 2001) or by enhancing the reverse transcription activity of the viral polymerase (Bouchard *et al.*, 2001; Klein *et al.*, 1999). Although it has been shown that the WHx protein is indispensable for virus replication *in vivo* (Zoulim *et al.*, 1994), which of the above functions is indispensable remains unknown. As HBV infects only humans and chimpanzees, it has been difficult to perform intensive studies *in vivo*.

Recently, Mercer *et al.* (2001) reported that transplanted human hepatocytes in SCID mice homozygous for the Alb-uPA transgene resulted in replacement of the mouse liver. They also reported that the highly replaced mice are susceptible to hepatitis C virus (Mercer *et al.*, 2001). Tateno *et al.* (2004) also created human hepatocyte chimeric mice with an improved replacement rate. Using this chimeric mouse model and the cell-culture-created HBV, we showed previously that hepatitis B e antigen (HBeAg) is dispensable for virus infection and replication (Tsuge *et al.*, 2005).

In this study, we tested whether the cell-culture-generated HBx-defective (HBx-def) HBV infects and replicates in the chimeric mice. As HBx-def HBV did not develop measurable viraemia, we expressed the HBx protein in the chimeric mouse liver by hydrodynamically injecting HBx-expression plasmid. It was noted that this *trans*-complementation of HBx helped the replication of HBx-def virus in the chimeric mice, and revertant viruses showed nucleotide substitutions that reversed the introduced stop codon [CAA to TAA created by a C-to-T point mutation at nt 1395 (aa 7) in the HBx gene; Fig. 1a] and restored expression. The HBx protein is thus indispensable for infection and proliferation of HBV. The protein thus might be a target for therapy development against HBV.

RESULTS

Production of HBV particles and antigens in cell culture and effect of HBx ablation

We initially examined nucleotide sequences of the cell-line-produced HBV by direct sequencing of the PCR products using cell-culture supernatants. As expected, HBV DNA was released from HepG2 cells transfected with the HBx-def plasmid with an introduced stop codon mutation by calcium phosphate precipitation (data not shown). We then analysed hepatitis B surface antigen (HBsAg), HBeAg and HBV DNA in the supernatants 3 days after transfection. While HBV DNA titres were not significantly different between the wild-type (WT)- and HBx-def HBV-transfected cultures, the HBsAg and the HBeAg levels were significantly lower in HBx-def HBV- than in WT-transfected cultures (Fig. 1b).

To examine the particle formation in the transfection experiments, we analysed the density of generated HBV by sucrose density gradient sedimentation analysis. The density of the cell-culture-produced HBx-def HBV was compared with those of WT HBV and HBV obtained from human serum. As shown in Fig. 1(c), each of the three preparations of HBV sedimented at sucrose density 1.18 g ml^{-1}, suggesting that cell-culture-produced HBV particles were similar to those obtained from human serum.

Infectivity of HBx-def HBV particles

To analyse the infectivity of HBx-def HBV, we inoculated cell-culture-produced recombinant HBV (WT HBV or HBx-def HBV) into chimeric mice. All seven mice injected with cell-culture-generated WT HBV developed measurable viraemia 2–7 weeks after inoculation. The virus titre reached 6–10 log_{10} copies ml^{-1} and the viraemia persisted for more than 4 months (Fig. 2a). In contrast, we did not observe any measurable viraemia in HBx-def HBV-injected mice within a period of 16 weeks after inoculation (Fig. 2b). Only five of 16 HBx-def HBV-inoculated mice became occasionally positive for HBV DNA by nested PCR assay. We then examined the mouse livers 14 weeks after inoculation by immunohistochemical staining with anti-HB core (HBc) antibody. As shown in Fig. 2(c), human hepatocytes of WT-injected mice were positive for HBV core antigen (HBcAg). In contrast, the staining was negative in mouse liver injected with HBx-def HBV.

Effect of *trans*-complementation of entire and partial HBx protein on replication of HBx-def HBV

We then investigated the effect of *trans*-complementation of the HBx protein both *in vitro* and *in vivo*. Since the C-terminal two-thirds (aa 51–154) domain of HBx has been reported to contain a transactivation domain (Tang *et al.*, 2005), we constructed three plasmids (full length and residues 1–50 and 51–154), as shown in Fig. 3(a). To analyse the effect of co-transfection of these three plasmids on intracellular replication of HBV, the cells transfected using *Trans*IT-LT1 reagent were harvested 24 h after transfection and analysed by Southern blotting. As shown in Fig. 3(b), *trans*-complementation of HBx enhanced the

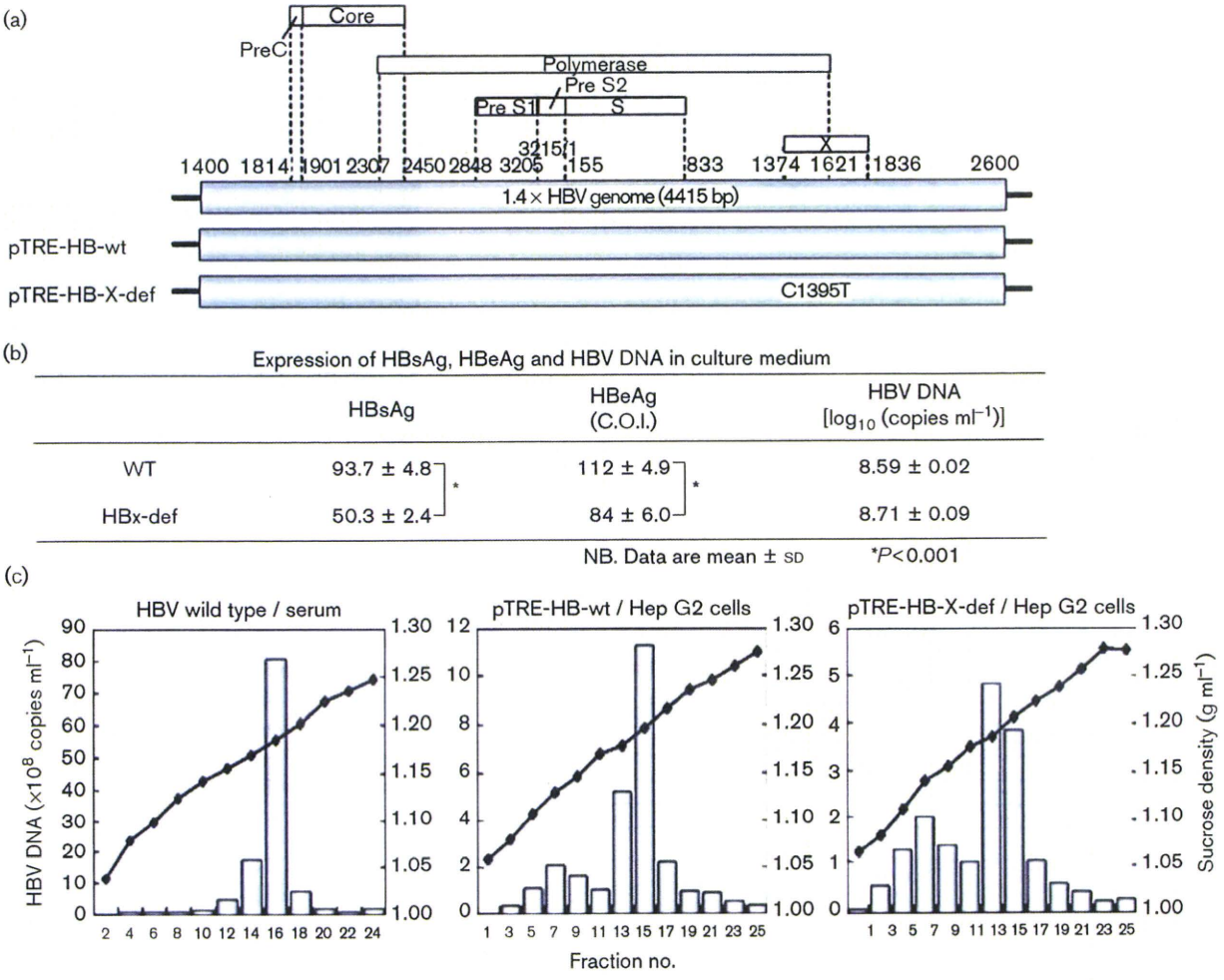

Fig. 1. Construction of HBV expression plasmids. (a) Wild type (WT) 1.4× genome length HBV was cloned into the pTRE2hyg vector (pTRE-HB-wt) and a nucleotide substitution, C1395T, was introduced to create the HBx-def mutant pTRE-HB-X-def. (b) Comparison of expression of HBsAg, HBeAg and HBV DNA in culture medium between WT and HBx-def. (c) Sucrose density gradient analysis of HBV particles (◆) and HBV DNA copies (bars) obtained from a serum sample (left) and supernatants from a cell culture transfected with WT HBV (pTRE-HB-wt, middle) and HBx-def pTRE-HB-X-def. C.O.I., cut-off index.

replication of HBV to the WT level. The effects of HBx protein were also evident on the expression of HBsAg (Fig. 3c) and HBeAg (Fig. 3d). As reported previously, the effect of the C-terminal two-thirds (aa 51–154) of the HBx protein was stronger than that of the entire protein and the N-terminal one-third (aa 1–50) (Tang *et al.*, 2005). The production of replication intermediates was increased similarly by co-transfection of the X proteins (Fig. 3e). To further study the effect of HBx expression, we analysed the levels of intracellular core protein expression. As shown in Fig. 4(a), the expression levels of the core protein were upregulated with the expression of the entire (WT) and C-terminal two-thirds (aa 51–154) of the HBx protein. Immunocytochemical analysis showed that only the cells with strong HBx protein expression were stained with the core protein (Fig. 4b). The core and HBx proteins in these cells were stained mainly in the cytoplasm.

Expression of HBx protein in mouse liver by hydrodynamic injection

Next, we expressed the HBx protein in the chimeric mouse liver with hydrodynamic injection. As shown in Fig. 5(a), a dose-dependent expression of the HBx protein with a haemagglutinin (HA) tag was confirmed by Western blot analysis. Although Henkler *et al.* (2001) showed an aggregation of HBx under the control of the human cytomegalovirus (CMV) promoter, we were able to observe expression of properly sized HBx. Immunohistochemical analysis also revealed HBx protein expression in the mouse

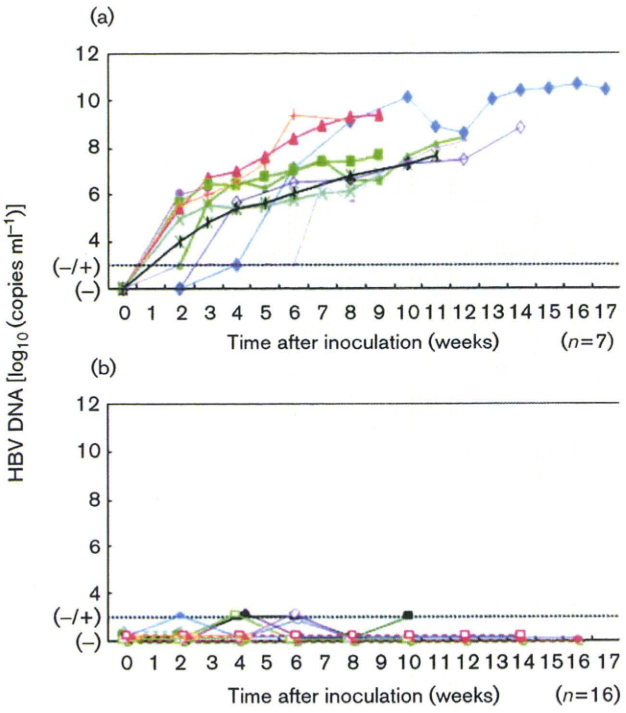

No. analysed mice

Weeks		2	4	6	8	10	12	14	16
HBV	(−/+)	1	3	3	0	1	0	0	0
DNA	(−)	15	10	6	9	6	5	5	3

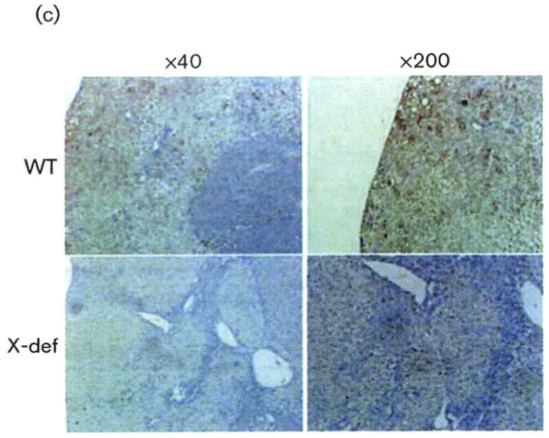

Fig. 2. Infection of human hepatocyte chimeric mice with cell-culture-derived HBV. (a, b) WT (a) and HBx-def (b) HBV particles generated from HepG2 cell lines by transfection of overlength HBV plasmid injected into chimeric mice. (c) Immunohistochemical analysis of mouse liver infected with WT (upper panel) and HBx-def (lower panel) HBV using anti-HBc antibody. HBV-infected hepatocytes were stained brown.

liver. Notably, the HBx protein staining was strong around the central vein (Fig. 5b).

Infection of HBx-def HBV particles with intrahepatic expression of the HBx protein

As the infection experiments with HBx-def HBV failed to result in measurable viraemia (Fig. 2b), we then tried to infect HBx-def HBV after expression of HBx protein by hydrodynamic injection. As shown in Fig. 6(a), six of seven mice developed measurable viraemia 2–8 weeks after inoculation. The incidence of measurable viraemia was significantly higher in mice that received hydrodynamic injection than in those without (Fig. 2b versus Fig. 6a, $P<0.0001$). Immunohistochemical analysis of the infected mice showed simultaneous staining for human serum albumin (hAlb) and HBcAg in the same portion of the liver (Fig. 6b).

Sequence analysis of inocula and the infected mouse sera

We analysed nucleotide sequences of the virus recovered from all six infected mice and compared them with those of inoculated HBx-def HBV. As shown in Fig. 7(a), direct sequencing analyses of the amplified HBV DNA products showed that all revertant viruses had T1395C (mouse MHX#1, 3, 5–7) or T1395A (mouse MHX#2) point mutations, which reverted the introduced stop codon to amino acids. We further analysed nucleotide sequences of HBV by cloning and sequencing using serum samples obtained from two mice (MHX#1, 33 clones; MHX#2, 38 clones) (Fig. 7b). Only one of 33 clones obtained from MHX#1 and none of the 38 clones from MHX#2 had the stop codon mutation that was introduced into the transfected plasmid.

DISCUSSION

In previous studies, HBx has been reported to be a multifunctional protein affecting cell growth and proliferation and activating transcription of mRNA (Arbuthnot *et al.*, 2000; Bouchard *et al.*, 2001; Klein *et al.*, 1999; Murakami, 2001) and virus replication in HCC cell lines (Bouchard *et al.*, 2001; Keasler *et al.*, 2007; Leupin *et al.*, 2005; Tang *et al.*, 2005) and mouse hepatocytes (Keasler *et al.*, 2007; Xu *et al.*, 2002). However, these results were obtained by introduction of HBV genomes into cells using artificial methods such as transfection, gene transfer and hydrodynamic injection. Recently, we established an *in vivo* HBV infection system using human hepatocyte chimeric mice (Tsuge *et al.*, 2005). The system enabled us to perform infection experiments using HBV-containing patient sera and cell-culture medium. Using this system,

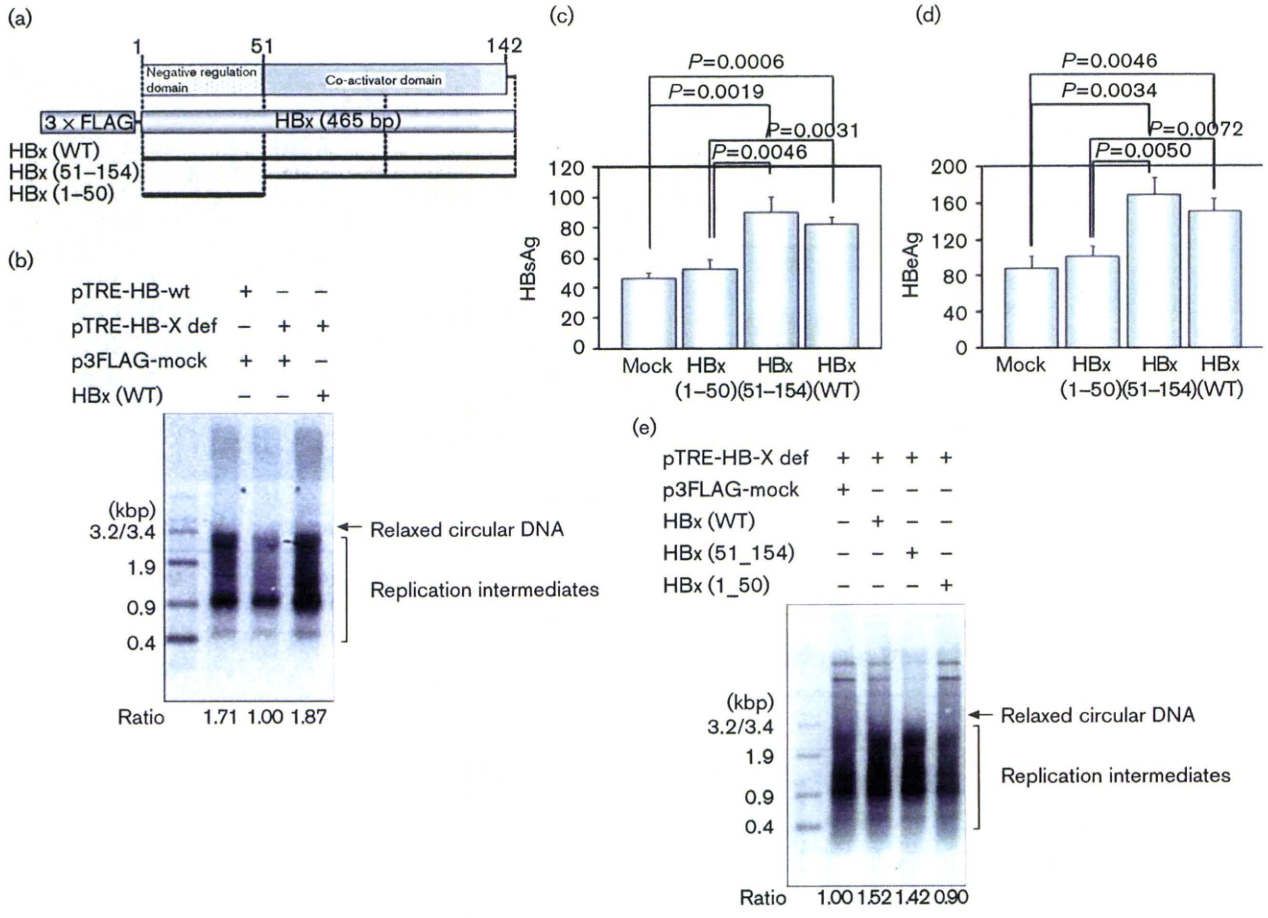

Fig. 3. Recovery of reduced formation of replication intermediate and HB antigens from HBx-def HBV by *trans*-complementation of HBx. (a) Construction of HBx expression plasmids. Full-length and deletion mutants of HBx gene were cloned into the p3FLAG-CMV10 or pcDNA3 or pcDNA3.1-3HA vector. Examples of three FLAG-tagged plasmids are shown. (b) *Trans*-complementation of HBx protein restored the reduced formation of replication intermediates of HBx-def HBV. The core-associated HBV replication intermediates were collected from HepG2 cells and detected with Southern blot hybridization with a full-length HBV probe. (c–e) Recovery of reduced production of HBsAg (c) and HBeAg (d) in culture medium and replication intermediates (e) of HBx-def HBV with *trans*-complementation of HBx expression plasmids. HBx (WT) and HBx(51–154), but not HBx(1–50), effectively enhanced the formation of HBV products. (b, e) The levels of core-associated HBV DNA are shown at the bottom of each lane. Data in (c) and (d) are mean ± SD of three experiments.

we showed previously that HBeAg is dispensable for HBV infection and active replication *in vivo* (Tsuge *et al.*, 2005). Virus replication following infection of HBV particles is quite similar to natural infection. We thus applied the system to study the function of HBx protein in this study. We also utilized hydrodynamic injection of HBx expression plasmid to *trans*-complement the defective HBx. As shown by Western blot analysis (Fig. 4a), HBx protein of the expected size was produced without development of antibody in this SCID-mouse-based model system.

This natural infection mode is quite different from previous animal studies. Virus titres of HBx-def HBV were approx. 50–99 % compared with WT HBV *in vitro* (Bouchard *et al.*, 2001; Keasler *et al.*, 2007; Leupin *et al.*, 2005; Tang *et al.*, 2005) and *in vivo* (Keasler *et al.*, 2007; Xu *et al.*, 2002). High-level HBx-def virus production seen in these experiments may be the result of expression of HBV proteins other than HBx following forced introduction of plasmids into mouse liver cells by hydrodynamic injection or transgenes. Such introduction probably resulted in virus production that is similar to *in vitro* transfection experiments using cultured cells.

In vitro experiments in this study showed that normal-density HBV particles (Fig. 1c) were produced in the absence of HBx. Curiously, the amount of HBV DNA released from the cells into the supernatant was not different between WT and HBx-def HBV, even though the

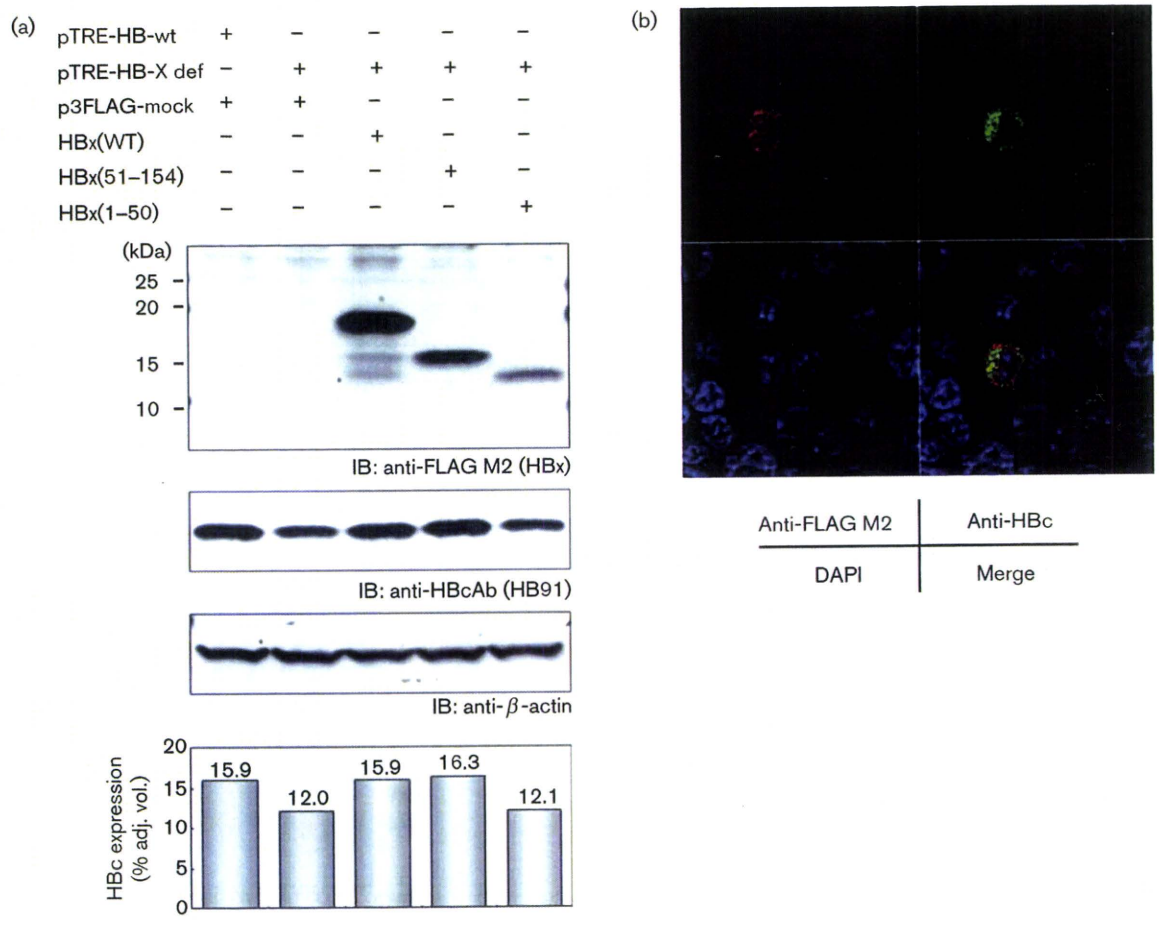

Fig. 4. Upregulation of intracellular core protein formation by *trans*-complementation of the HBx proteins. (a) Western blot analysis of intracellular proteins. Expression of the HBx proteins (percentage adjusted volume) is shown by staining the fused FLAG tag (upper panel). The membrane was also stained by the anti-HBc (middle) and anti-β-actin (lower) antibodies. Values obtained by scanning via densitometer are shown at the bottom of each lane. (b) Immunohistochemical analysis of HepG2 cells co-transfected with pTRE2-HB-X-def and p3FLAG-HBx plasmids. The expression of HBx and HBc proteins was detected by anti-FLAG (upper left) and anti-HBc (upper right) antibody, respectively. The merged image is shown in the lower right and nuclei are shown in the lower left panel. Note that only cells positive for HBx are also positive for HBc protein.

amounts of HBsAg and HBeAg as well as the amount of HBV DNA in cells were significantly greater in WT (Fig. 1b). Efficacy of release of the virus from the cells might be different between WT and HBx-def HBV. Alternatively, production of defective virus, which appeared as the second peak of HBV DNA in the sucrose gradient experiment (Fig. 1c, right panel), might be enriched in HBV DNA in the supernatant of HBx-def HBV. The reason for this discrepancy is unknown. Previous papers did not mention such production of HBV into the supernatant.

Similarly, in the absence of HBx protein *in vitro*, the formation of the replication intermediates (Fig. 3) and production of intracellular core protein (Fig. 4) continued, although their amounts were much lower. It is thus difficult to explain the inability of HBx-def HBV to infect *in vivo* simply from its transcription-activating ability, although our results confirmed that HBx has *trans*-activation ability, as reported previously (Keasler *et al.*, 2007; Tang *et al.*, 2005; Xu *et al.*, 2002). A different mode of introduction of viral nucleic acid might explain the difference seen in *in vitro* and *in vivo* experiments. In the transfection experiments, a relatively large amount of HBV DNA is introduced by transfection. In contrast, only successfully attached virus particles can introduce viral DNA into liver cells.

Strikingly, all but one (70 of 71 clones) revertant viruses had nucleotide substitutions that reversed the introduced stop codon to a coding amino acid. This is in contrast to the fact that HBV replicates in the HBx-def form in cultured cells, even though the efficacy is lower than in WT. We assumed that complemented HBx protein stimulated the replication of HBx-def HBV and increased the chance of nucleotide sequence substitutions in the HBx

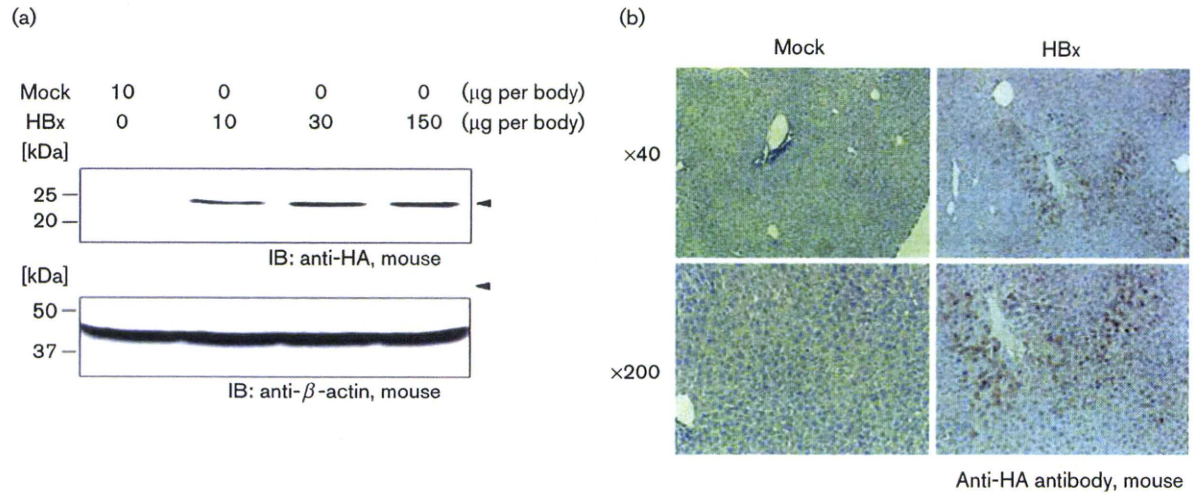

Fig. 5. Expression of HBx protein by hydrodynamic injection of HBx plasmid. (a) Liver-expressed HA-tagged HBx proteins were detected by Western blot analysis using anti-HA antibody (HA tag was used to avoid non-specific binding of anti-FLAG tag to mouse liver proteins). Dose-dependent expression of the protein was observed with different doses of the injected plasmid. (b) Immunohistochemical analysis of mouse liver using anti-HA antibody revealing expression of HBx protein. The protein was mainly expressed around the central vein.

gene, and that only revertant HBV variants predominantly increased, due to their rapid replication ability through the infection–replication cycle that only exists in the *in vivo* model. One might consider the possibility that the HBx protein works as a mutagen. However, we did not observe clear differences in the incidence of nucleotide sequence substitutions between the presence and absence of HBx (Fig. 7b and data not shown).

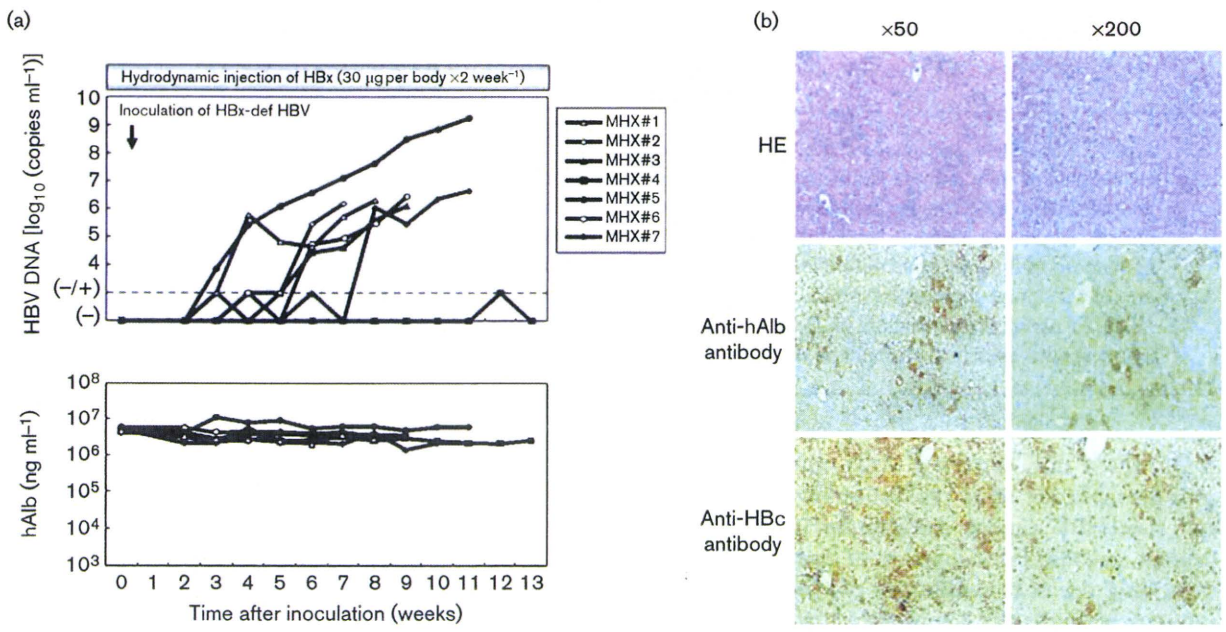

Fig. 6. Infection of HBx-def HBV particles after hydrodynamic injection of HBx expression plasmid. (a) Full-length HBx protein expression plasmid was hydrodynamically injected twice a week into human hepatocyte chimeric mice. Two weeks after the beginning of the injections, cell-culture-derived HBx-def HBV particles were injected through the tail vein. HBV DNA (upper panel) and hAlb (lower panel) were measured. (b) Immunohistochemical analysis of the infected mouse. The liver was stained with haematoxylin and eosin (HE) (upper), antibody against hAlb (middle) and anti-HBc antibody (lower).

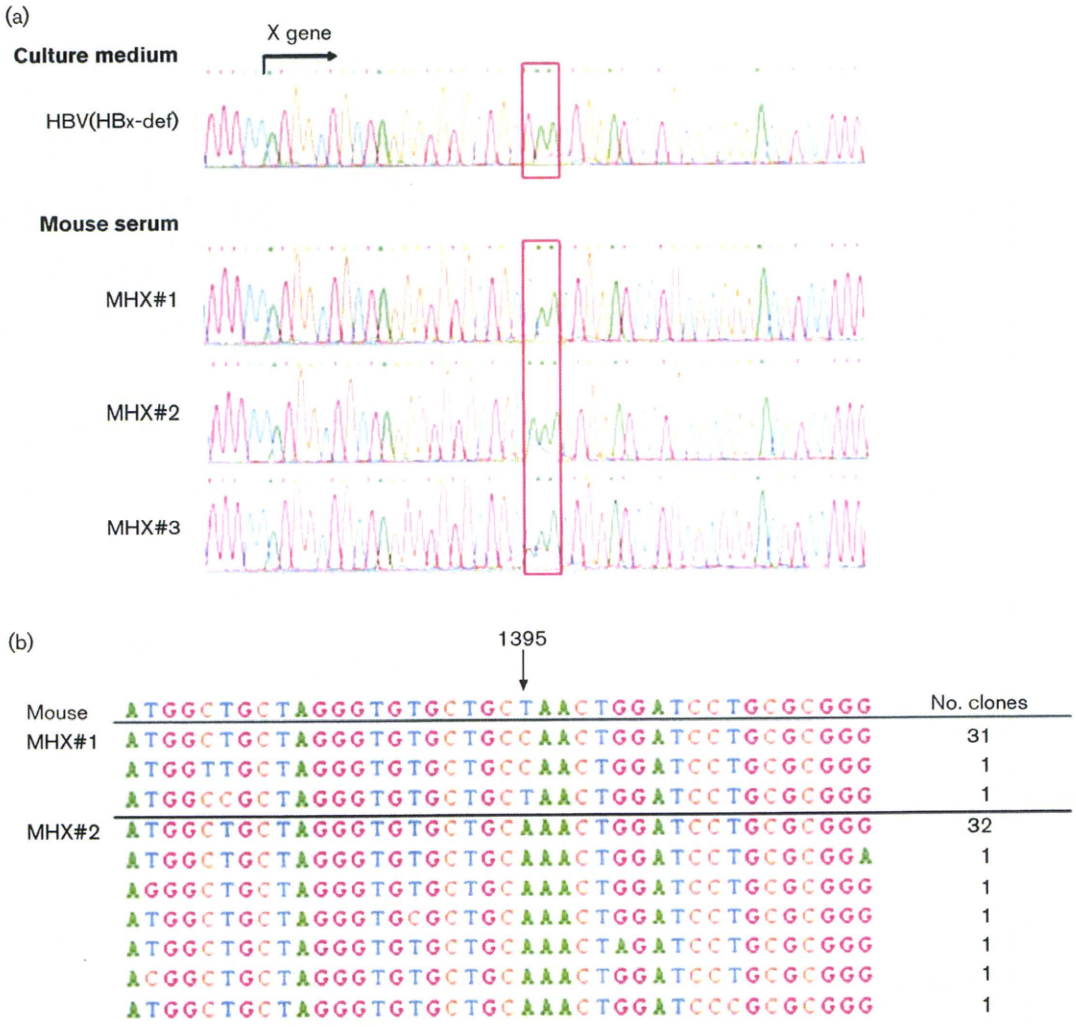

Fig. 7. Nucleotide sequence analysis of HBV recovered from HBx-def HBV-injected mice. (a) Nucleotide sequences of the HBx region of HBV determined by direct sequencing of PCR products using serum samples obtained from three mice (#1, #2 and #3 in Fig. 6a). The sequences were compared with that of inoculated HBV. Note that one of the three mice (#2) had a unique sequence different from the original sequence before introduction of the stop codon (C1395T). (b) Nucleotide sequences of the HBx gene determined by cloning and sequencing of PCR-amplified DNA from mice #1 and #2. Note that only one of 63 clones showed the introduced stop codon mutation. As we used a large amount of HBV plasmids, special care was taken to avoid contamination of DNA. Water was used as a negative control for all experiments and we observed no inappropriate amplification in these experiments.

It is thus still uncertain why the HBx protein is indispensable for virus replication *in vivo*. However, the fact that HBV cannot replicate in the absence of HBx protein may allow development of therapeutic medicine by disturbing the unknown action of HBx. To this end, it is interesting to identify a substance that binds to HBx.

The indispensability of the X protein for virus replication is a common feature shared by HBV and WHV (Chen *et al.*, 1993; Zoulim *et al.*, 1994). Both of them cause chronic infection, inflammation, fibrosis and cancer. In contrast, DHBV, which can replicate without DHBx expression, does not cause such a pathological situation (Meier *et al.*, 2003). Further analysis of the X protein may pave the way to clarify the mechanism of cancer development caused by HBV infection.

METHODS

Human hepatocyte chimeric mice experiments. Care of uPA$^{+/+}$/SCID$^{+/+}$ mice and transplantation of human hepatocytes were performed as described previously (Tateno *et al.*, 2004). The experiments were performed in accordance with the guidelines of the local committee for animal experiments at Hiroshima University. Infection, extraction of serum samples and sacrifice were performed under ether anaesthesia as described previously (Tateno *et al.*, 2004).

hAlb in mouse serum was measured with a Human Albumin ELISA Quantification kit (Bethyl Laboratories Inc.) according to the instructions provided by the manufacturer. Serum samples obtained from mice were aliquotted and stored in liquid nitrogen until use.

Analysis of HBV markers. HBsAg and HBeAg were measured using a commercially available ELISA kit (Abbott). For quantitative analysis of HBV DNA, 10 μl mouse serum sample or 100 μl of culture supernatant was used. DNA was extracted from these samples using the SMITEST R&D (Genome Science Laboratories) and dissolved in 20 μl H_2O, and HBV DNA was quantified by real-time PCR using the 7300 Real-Time PCR System (Applied Biosystems). Amplification was performed as described previously (Tsuge *et al.*, 2005). The lower detection limit of this assay is 300 copies. For detection of small amounts of HBV DNA, we also performed nested PCR. The amplification conditions were as described previously (Tsuge *et al.*, 2005).

Plasmid construction. The construction of wild-type (WT) HBV 1.4 genome length, pTRE-HB-wt, was described previously (Tsuge *et al.*, 2005). We used pTRE2 vector without pTet-off vector and doxycycline because a sufficient amount of HBV transcripts was produced from internal HBV promoters, and transcription from the pTRE2 promoter is negligible under these conditions. The nucleotide sequence of the HBV genome that we cloned into plasmid pTRE-HB-wt was deposited in GenBank under accession number AB206817. A modified plasmid, pTRE-HB-X-def, was generated by introducing a C-to-T point mutation at nt 1395 (aa 7) to create a stop codon (CAA to TAA) in the HBx gene (Fig. 1a). The substitution was introduced by using a QuikChange Site-Directed Mutagenesis kit (Stratagene). For the construction of the HBx gene expression plasmid, the HBx gene was amplified from pTRE-HB-wt and cloned into pcDNA3, pcDNA3-3 × HA, p3 × FLAG-CMV10 vectors and designated pcDNA-HBx, pcDNA3-HA-HBx, p3FLAG-HBx, respectively. Partially truncated HBx plasmids, with a deletion of the N-terminal 50 aa [HBx(51–154)] and the C-terminal 50 aa [HBx(1–50)], were also cloned into pcDNA3 or p3FLAG-CMV10 vectors.

Transfection of HepG2 cell lines with HBV expression plasmids. HepG2 cells were grown in Dulbecco's modified Eagle's medium supplemented with 10 % (v/v) fetal bovine serum at 37 °C and under 5 % CO_2. For functional analysis of the HBx protein *in vitro*, the HBV or HBx-def HBV expression plasmid was transfected with/without HBx expression plasmid using *Trans*IT-LT1 (Mirus) reagent according to the instructions provided by the supplier. Three to five days after transfection, core-associated HBV DNA was extracted from cells for HBV DNA quantification (Noguchi *et al.*, 2005). For analysing the infectivity of recombinant HBV particles, HBV expression plasmids were transiently transfected into HepG2 cells. The cells were seeded to semi-confluence in 90 mm dishes. WT HBV particles were generated from cells transfected with 20 μg pTRE2-HB-wt by calcium phosphate precipitation. HBx-def HBV particles were also generated from cells co-transfected with 10 μg pTRE2-HB-X-def and 10 μg pcDNA-HBx. Three days after transfection, the culture medium was collected and stored in liquid nitrogen until use.

Analysis of cell-culture-produced HBV by sucrose density gradient sedimentation. Five millilitres of HBV-positive human serum (8 $\log_{10}$ copies ml^{-1}) or 50 ml cell culture supernatant (8 $\log_{10}$ copies ml^{-1}) was layered on a 20 % (w/w) sucrose cushion, and centrifuged at 24 000 r.p.m. (maximum 103 864 *g*) for 12 h at 4 °C with a Beckman SW28 rotor (Beckman Coulter). The precipitate was resuspended in 500 μl PBS. These HBV samples were layered on a linear 20–50 % (w/w) sucrose gradient. Centrifugation was carried out at 24 000 r.p.m. (maximum 102 445 *g*) for 21 h at 4 °C with a Beckman SW40 rotor. The gradients were fractionated into 500 μl samples, and the density of each fraction was calculated from the weight and volume. Each fraction was diluted 10-fold and tested for HBV DNA by real-time PCR.

Analysis of replication intermediate of HBV. The cells were harvested 5 days after transfection and lysed with 250 μl lysis buffer [10 mM Tris/HCl (pH 7.4), 140 mM NaCl and 0.5 % (v/v) NP-40] followed by centrifugation for 2 min at 15 000 *g*. The core-associated HBV genome was immunoprecipitated by mouse anti-HBV core monoclonal antibody 2A21 (Institute of Immunology, Tokyo, Japan) and subjected to Southern blot analysis after SDS/proteinase K digestion, followed by phenol extraction and ethanol precipitation. Quantitative analysis was performed by real-time PCR with SYBR Green using the 7300 Real-Time PCR System and the amounts of the replication intermediates were compared. The HBV-specific primers used for amplification were 5′-TTTGGGCATGGACATTGAC-3′ and 5′-GGTGAACAATGTTCCGGAGAC-3′. The amplification conditions included initial denaturation at 95 °C for 10 min, followed by 45 cycles of denaturation at 95 °C for 15 s, annealing at 58 °C for 5 s and extension at 72 °C for 6 s. The lower detection limit of this assay was 300 copies.

Immunocytochemistry of HepG2 cells transfected with pTRE2-HB-X-def and p3FLAG-HBx plasmids. HepG2 cells were seeded to semi-confluence in two-well chamber plates. Each 1 μg pTRE2-HB-X-def and p3FLAG-HBx plasmids was co-transfected using *Trans*IT-LT1 reagent (Mirus) according to the instructions provided by the supplier. The cells were harvested 24 h after transfection and then washed with PBS and fixed with 4 % (v/v) paraformaldehyde. After fixation, the cells were stained with mouse monoclonal antibody directed to FLAG (Sigma) or rabbit polyclonal antibody against hepatitis B core antigen (HBcAg; DAKO Diagnostika) as the primary antibody. The bound antibodies were detected with an Alexa Fluor 488-conjugated antibody against rabbit IgG or Alexa Fluor 568-conjugated antibody against mouse IgG, respectively (Molecular Probes). Nuclei were counterstained with 6-diamidino-2-phenylindole (DAPI) (Vector Laboratories).

Hydrodynamic injection of HBx expression plasmids. Hydrodynamic injection was performed as reported previously (Yang *et al.*, 2002) with slight modifications. As the human hepatocyte chimeric mice were quite small (12–15 g) and weak for the rapid injection and the stress, we reduced the amount of DNA solution and injection speed: 1 ml PBS containing 30 μg HBx expression plasmids was injected rapidly through the mouse tail vein within 30 s. For analysis of infectivity of HBx-def HBV particles, the plasmids were injected twice a week.

Western blot analysis. Mouse liver tissues or transfected HepG2 cells were cooled on ice and treated with RIPA-like buffer [50 mM Tris/HCl (pH 8.0), 0.1 % SDS, 1 % NP-40, 150 mM sodium chloride and 0.5 % sodium deoxycholate] containing protease inhibitor cocktail (Sigma). Cell lysates were separated on SDS–polyacrylamide gels [5–20 % (w/v)] (Bio-Rad) and then transferred onto nitrocellulose membranes (GE Healthcare) by electroblotting. The membranes were incubated with anti-haemagglutinin fusion epitope (anti-HA) monoclonal antibody (Roche) or with anti β-actin monoclonal antibody (Sigma) followed by incubation with horseradish peroxidase-conjugated sheep anti-mouse immunoglobulin (GE Healthcare). Proteins were visualized via the ChemiDoc XRS system (Bio-Rad). Expression of HBc protein was quantified from the densities of the immunoblot signals by Quantity One software (Bio-Rad).

Immunohistochemical analysis of mouse liver. The liver specimens of HBV-infected mice were fixed with 10 % buffered paraformaldehyde and embedded in paraffin blocks for histological

examination. The liver sections were stained with haematoxylin–eosin or subjected to immunohistochemical staining using an antibody against HBcAg (DAKO Diagnostika), anti-HA antibody or HSA (Bethyl Laboratories Inc.). Endogenous peroxidase activity was blocked with 0.3% H_2O_2 and methanol. Immunoreactive materials were visualized by using a streptavidin–biotin staining kit (Histofine SAB-PO kit; Nichirei) and diaminobenzidine.

Sequence analysis of the HBV genome. Genome-length HBV DNA was amplified by PCR as described by Günther *et al.* (1995). HBV genome-length PCR products were subjected to 1% agarose gel electrophoresis and the 3.2 kbp band was extracted using a QiaEx II Gel Extraction kit (Qiagen). Direct sequencing, cloning and sequencing (Ohishi *et al.*, 2004) were performed in an ABI PRISM 3100-Avant Genetic Analyzer (Applied Biosystems) with a Big Dye Terminator version 3.0 Cycle Sequencing Ready Reaction kit (Applied Biosystems).

Statistical analysis. All data are expressed as mean ± SD. Differences between groups were examined for statistical significance by using Student's *t*-test. A P value <0.05 denoted the presence of a statistically significant difference.

ACKNOWLEDGEMENTS

This work was carried out at the Research Center for Molecular Medicine, Faculty of Medicine, Hiroshima University, and the Analysis Center of Life Science, Hiroshima University. The authors thank Chiemi Noguchi and Waka Ohishi for their helpful discussion, Kana Kunihiro for her excellent technical assistance, and Yoshiko Nakata and Aya Furukawa for secretarial assistance. Financial support was provided by the Ministry of Education, Sports, Culture and Technology and Ministry of Health, Labour and Welfare (Grants-in-Aid for scientific research and development).

REFERENCES

Ando, T., Sugiyama, K., Goto, K., Miyake, Y., Li, R., Kawabe, Y. & Wada, Y. (1999). Age at time of hepatitis Be antibody seroconversion in childhood chronic hepatitis B infection and mutant viral strain detection rates. *J Pediatr Gastroenterol Nutr* 29, 583–587.

Arbuthnot, P., Capovilla, A. & Kew, M. (2000). Putative role of hepatitis B virus X protein in hepatocarcinogenesis: effects on apoptosis, DNA repair, mitogen-activated protein kinase and JAK/STAT pathways. *J Gastroenterol Hepatol* 15, 357–368.

Bouchard, M. J., Wang, L. H. & Schneider, R. J. (2001). Calcium signaling by HBx protein in hepatitis B virus DNA replication. *Science* 294, 2376–2378.

Chen, H. S., Kaneko, S., Girones, R., Anderson, R. W., Hornbuckle, W. E., Tennant, B. C., Cote, P. J., Gerin, J. L., Purcell, R. H. & Miller, R. H. (1993). The woodchuck hepatitis virus X gene is important for establishment of virus infection in woodchucks. *J Virol* 67, 1218–1226.

Colgrove, R., Simon, G. & Ganem, D. (1989). Transcriptional activation of homologous and heterologous genes by the hepatitis B virus X gene product in cells permissive for viral replication. *J Virol* 63, 4019–4026.

Dandri, M., Schirmacher, P. & Rogler, C. E. (1996). Woodchuck hepatitis virus X protein is present in chronically infected woodchuck liver and woodchuck hepatocellular carcinomas which are permissive for viral replication. *J Virol* 70, 5246–5254.

Dandri, M., Petersen, J., Stockert, R. J., Harris, T. M. & Rogler, C. E. (1998). Metabolic labeling of woodchuck hepatitis B virus X protein in naturally infected hepatocytes reveals a bimodal half-life and association with the nuclear framework. *J Virol* 72, 9359–9364.

Doria, M., Klein, N., Lucito, R. & Schneider, R. J. (1995). The hepatitis B virus HBx protein is a dual specificity cytoplasmic activator of Ras and nuclear activator of transcription factors. *EMBO J* 14, 4747–4757.

Ganem, D. & Schneider, R. J. (2001). *Hepadnaviridae*: the viruses and their replication. In *Fields Virology*, 4th edn, pp. 2923–2969. Edited by D. M. Knipe, P. M. Howley, D. E. Griffin, R. A. Lamb, M. A. Martin, B. Roizman & S. E. Straus. Philadelphia, PA: Lippincott Williams & Wilkins.

Günther, S., Li, B. C., Miska, S., Kruger, D. H., Meisel, H. & Will, H. (1995). A novel method for efficient amplification of whole hepatitis B virus genomes permits rapid functional analysis and reveals deletion mutants in immunosuppressed patients. *J Virol* 69, 5437–5444.

Henkler, F., Hoare, J., Waseem, N., Goldin, R. D., McGarvey, M. J., Koshy, R. & King, I. A. (2001). Intracellular localization of the hepatitis B virus HBx protein. *J Gen Virol* 82, 871–882.

Jacob, J. R., Ascenzi, M. A., Roneker, C. A., Toshkov, I. A., Cote, P. J., Gerin, J. L. & Tennant, B. C. (1997). Hepatic expression of the woodchuck hepatitis virus X-antigen during acute and chronic infection and detection of a woodchuck hepatitis virus X-antigen antibody response. *Hepatology* 26, 1607–1615.

Keasler, V. V., Hodgson, A. J., Madden, C. R. & Slagle, B. L. (2007). Enhancement of hepatitis B virus replication by the regulatory X protein *in vitro* and *in vivo*. *J Virol* 81, 2656–2662.

Klein, N. P., Bouchard, M. J., Wang, L. H., Kobarg, C. & Schneider, R. J. (1999). Src kinases involved in hepatitis B virus replication. *EMBO J* 18, 5019–5027.

Leupin, O., Bontron, S., Schaeffer, C. & Strubin, M. (2005). Hepatitis B virus X protein stimulates viral genome replication via a DDB1-dependent pathway distinct from that leading to cell death. *J Virol* 79, 4238–4245.

Meier, P., Scougall, C. A., Will, H., Burrell, C. J. & Jilbert, A. R. (2003). A duck hepatitis B virus strain with a knockout mutation in the putative X ORF shows similar infectivity and *in vivo* growth characteristics to wild-type virus. *Virology* 317, 291–298.

Melegari, M., Wolf, S. K. & Schneider, R. J. (2005). Hepatitis B virus DNA replication is coordinated by core protein serine phosphorylation and HBx expression. *J Virol* 79, 9810–9820.

Mercer, D. F., Schiller, D. E., Elliott, J. F., Douglas, D. N., Hao, C., Rinfret, A., Addison, W. R., Fischer, K. P., Churchill, T. A. & other authors (2001). Hepatitis C virus replication in mice with chimeric human livers. *Nat Med* 7, 927–933.

Murakami, S. (2001). Hepatitis B virus X protein: a multifunctional viral regulator. *J Gastroenterol* 36, 651–660.

Noguchi, C., Ishino, H., Tsuge, M., Fujimoto, Y., Imamura, M., Takahashi, S. & Chayama, K. (2005). G to A hypermutation of hepatitis B virus. *Hepatology* 41, 626–633.

Ohishi, W., Shirakawa, H., Kawakami, Y., Kimura, S., Kamiyasu, M., Tazuma, S., Nakanishi, T. & Chayama, K. (2004). Identification of rare polymerase variants of hepatitis B virus using a two-stage PCR with peptide nucleic acid clamping. *J Med Virol* 72, 558–565.

Raney, A. K. & McLachlan, A. (1991). The biology of hepatitis B virus. In *Molecular Biology of the Hepatitis B Virus*, pp. 1–37. Edited by A. McLachlan. Boca Raton, FL: CRC Press.

Seeger, C. & Mason, W. S. (2000). Hepatitis B virus biology. *Microbiol Mol Biol Rev* 64, 51–68.

Sitterlin, D., Bergametti, F., Tiollais, P., Tennant, B. C. & Transy, C. (2000a). Correct binding of viral X protein to UVDDB-p127 cellular protein is critical for efficient infection by hepatitis B viruses. *Oncogene* 19, 4427–4431.

Sitterlin, D., Bergametti, F. & Transy, C. (2000b). UVDDB p127-binding modulates activities and intracellular distribution of hepatitis B virus X protein. *Oncogene* **19**, 4417–4426.

Su, Q., Schroder, C. H., Hofmann, W. J., Otto, G., Pichlmayr, R. & Bannasch, P. (1998). Expression of hepatitis B virus X protein in HBV-infected human livers and hepatocellular carcinomas. *Hepatology* **27**, 1109–1120.

Tang, H., Banks, K. E., Anderson, A. L. & McLachlan, A. (2001). Hepatitis B virus transcription and replication. *Drug News Perspect* **14**, 325–334.

Tang, H., Delgermaa, L., Huang, F., Oishi, N., Liu, L., He, F., Zhao, L. & Murakami, S. (2005). The transcriptional transactivation function of HBx protein is important for its augmentation role in hepatitis B virus replication. *J Virol* **79**, 5548–5556.

Tateno, C., Yoshizane, Y., Saito, N., Kataoka, M., Utoh, R., Yamasaki, C., Tachibana, A., Soeno, Y., Asahina, K. & other authors (2004). Near completely humanized liver in mice shows human-type metabolic responses to drugs. *Am J Pathol* **165**, 901–912.

Tsuge, M., Hiraga, N., Takaishi, H., Noguchi, C., Oga, H., Imamura, M., Takahashi, S., Iwao, E., Fujimoto, Y. & other authors (2005). Infection of human hepatocyte chimeric mouse with genetically engineered hepatitis B virus. *Hepatology* **42**, 1046–1054.

Wang, W. L., London, W. T. & Feitelson, M. A. (1991). Hepatitis B X antigen in hepatitis B virus carrier patients with liver cancer. *Cancer Res* **51**, 4971–4977.

Xu, Z., Yen, T. S., Wu, L., Madden, C. R., Tan, W., Slagle, B. L. & Ou, J. H. (2002). Enhancement of hepatitis B virus replication by its X protein in transgenic mice. *J Virol* **76**, 2579–2584.

Yang, P. L., Althage, A., Chung, J. & Chisari, F. V. (2002). Hydrodynamic injection of viral DNA: a mouse model of acute hepatitis B virus infection. *Proc Natl Acad Sci U S A* **99**, 13825–13830.

Zhang, Z., Torii, N., Hu, Z., Jacob, J. & Liang, T. J. (2001). X-deficient woodchuck hepatitis virus mutants behave like attenuated viruses and induce protective immunity *in vivo*. *J Clin Invest* **108**, 1523–1531.

Zoulim, F., Saputelli, J. & Seeger, C. (1994). Woodchuck hepatitis virus X protein is required for viral infection *in vivo*. *J Virol* **68**, 2026–2030.

Journal of Surgical Research ■, e1–e9 (2011)
doi:10.1016/j.jss.2010.12.008

Therapeutic Potential of Propagated Hepatocyte Transplantation in Liver Failure

Hironobu Amano, M.D.,* Hiroshi Hino, M.D.,* Chise Tateno, Ph.D.,† Kentaro Emoto, M.D.,* Yasuhiro Imaoka, M.D.,* Chihiro Yamasaki, Ph.D.,‡ Toshiyuki Itamoto, M.D.,* Hirotaka Tashiro, M.D.,* Toshimasa Asahara, M.D.,* Hideki Ohdan, M.D.,* and Katsutoshi Yoshizato, Ph.D.†‡§,[1]

*Department of Surgery, Division of Frontier Medical Science, Programs for Biomedical Research, Graduate School of Biomedical Sciences, Hiroshima University, Hiroshima, Japan; †PhoenixBio, Co., Ltd., Hiroshima, Japan; ‡Yoshizato Project, CLUSTER, Prefectural Institute of Industrial Science and Technology, Hiroshima, Japan; and §Osaka City University Graduate School of Medicine, Osaka, Japan

Submitted for publication July 18, 2010

Background. **This study aimed to evaluate the therapeutic potential of intrasplenic transplantation of culture-propagated homologous hepatocytes in rats suffering from acute liver failure (ALF).**

Methods. **ALF was induced in dipeptidyl peptidase IV-negative (DPPIV$^-$) Fischer 344 rats by totally removing the two anterior liver lobes (68% of the liver) and ligating the pedicle of the right lobe (24% of the liver). Hepatocytes isolated from DPPIV$^+$ Fischer 344 rats were cultured for 11 d to propagate 3-fold, and the resulting hepatocytes were dubbed "culture-propagated hepatocytes (CPHEPs)". A total of 1.5×10^7 cells of CPHEPs were transplanted intrasplenically before ALF induction (CPHEP group). Similarly, freshly isolated hepatocytes (FIHEPs) were transplanted as a positive control (FIHEP group), and culture medium (CM) was injected into rats as a negative control (CM group).**

Results. **The survival of the CPHEP group was comparable to that of the FIHEP group and longer than that of the CM group ($P < 0.01$). Both CPHEP and FIHEP transplantation improved blood parameters such as ammonia, total bilirubin, glutamic pyruvic transaminase, and glutamic oxaloacetic transaminase; transplantation also affected liver tissue parameters such as apoptosis rate and bromodeoxyuridine-labeling index.**

Conclusions. **Transplantation of culture-propagated homologous hepatocytes has a remarkable therapeutic potential for ALF in rats.**

[1] To whom correspondence and reprint requests should be addressed at PhoenixBio, Co., Ltd., 3-4-1 Kagamiyama, Higashihiroshima, Hiroshima 739-0046, Japan. E-mail: katsutoshi.yoshizato@phoenixbio.co.jp.

Key Words: **dipeptidyl peptidase IV mutant rats; intrasplenic transplantation; omental lobe; apoptosis; histopathology; hepatectomy.**

INTRODUCTION

Orthotopic liver transplantation (OLT) has been proven to be an effective treatment for acute liver failure (ALF) [1–3]. However, the availability of donor organs for OLT is severely limited. Hepatocyte transplantation, which could provide a solution to donor organ shortages, has potential advantages over OLT [4].

The development of the hepatocyte transplantation technology over the past two decades reflects the progress of basic studies on human hepatocytes. Several patients have received hepatocyte transplantation as treatment for ALF to either give the native liver time to recover or serve as a bridge to liver transplantation [5–7]. However, there is a shortage of human hepatocytes for transplantation, which requires us to develop technology for repeatedly multiplying normal human hepatocytes *in vitro*.

Previously, we devised a new culture method by which adult rat and human hepatocytes could be maintained/propagated for up to at least 1 mo, repeatedly dividing and showing a bipotential differentiation capacity [8–11]. These highly replicative hepatocytes were isolated from liver tissues as "small hepatocytes" and were cultured in a new culture medium (hepatocyte clonal growth medium [HCGM]). The proliferative

0022-4804/$36.00

hepatocytes under culture expressed normal differentiated hepatocytic phenotypes and retained normal liver functions, including albumin (Alb) secretion and lidocaine and D-galactose metabolization. We dubbed these hepatocytes propagated *in vitro* as "culture-propagated hepatocytes" (CPHEPs). In the present study, we demonstrate that transplantation of homologous CPHEPs to a rat model of ALF improves its survival.

MATERIAL AND METHODS

Animals

Two types of Fischer 344 rats were used in the present study: wild-type with respect to the dipeptidyl peptidase IV (DPPIV) gene, DPPIV-positive ($DPPIV^+$), and its mutant, DPPIV-negative ($DPPIV^-$). Ten-wk-old wild-type rats, weighing 220 g, were purchased from the Shizuoka Laboratory Animal Center (Shizuoka, Japan), and age-matched mutant female rats, weighing 140 g, were obtained from Charles River Japan, Inc. (Kanagawa, Japan). They were housed in accordance with the criteria outlined in the *Guide for the Care and Use of Laboratory Animals*, prepared by the National Academy of Science.

Preparation of Cells

Hepatocytes were separated from the rats by the two-step collagenase perfusion method [12, 13] . Their viability, as measured by the trypan blue exclusion test, was more than 90%. The hepatocytes were then suspended in Dulbecco's modified Eagle's medium (DMEM; Gibco BRL, Life Technologies Inc., Rockville, MD)—containing 10% fetal bovine serum (FBS; HyClone Laboratories Inc., Logan, UT), 20 mM/L HEPES (Gibco BRL), 44 mmol/L $NaHCO_3$, and antibiotics (100 IU/mL penicillin G and 100 μg/mL streptomycin; Gibco BRL)—and were used as freshly isolated hepatocytes (FIHEPs) in transplantation experiments.

Aliquots of FIHEPs were inoculated at 8.5×10^3 cells/cm^2 in HCGM; 24 h later, they were cocultured with Swiss 3T3 cells (American Type Culture Collection, Rockville, MD) at a density of 8.5×10^3 cells/cm^2 treated with 10 μg/mL mitomycin C (Sigma-Aldrich, Tokyo, Japan), as reported previously [8–10]. The culture was maintained for 11 d to allow cell proliferation, with medium changes every 3 d for the first 9 d. The resulting cells were used as CPHEPs in transplantation experiments. In the preliminary experiments, we investigated the growth kinetics and viability of the hepatocytes during primary and secondary culture. The hepatocytes progressively expanded and reached the culture confluent state 11 d after commencing the culture. During primary culture, the viability of the expanded hepatocytes was well maintained. After secondary culture, however, the growth of the hepatocytes was rather limited and their viability was not well maintained. Based on these results, we used hepatocytes cultivated for 11 d for treatment in this study. Other aliquots of FIHEPs were suspended in DMEM, subjected to more than three times warming/freezing (liquid nitrogen) cycle, and used as "dead hepatocytes" (DHEPs). Single-passaged syngeneic rat fibroblasts (FBs) were cultured for 10 d and used for transplantation experiments.

Induction of ALF

The surgical animal ALF model [14, 15] was used as the host for the transplantation experiments. After laparotomy, the common pedicle to the right lobes was ligated, and the two anterior liver lobes were removed [16], leaving the omental lobes intact.

Hepatocyte Transplantation

FIHEPs and CPHEPs were each suspended in 0.3 mL DMEM and were individually transplanted into the spleen using a 27-gauge needle (TERUMO, Tokyo, Japan). $DPPIV^-$ rats were used as recipients, and hepatocytes from the wild-type ($DPPIV^+$) counterparts were used as donor cells to distinguish donor cells from host cells [13, 17]. Control group animals were injected with culture medium (CM group). The same numbers of DHEPs and rat FBs were similarly transplanted into the spleen. Thus, in the present study, there were five groups of rats: the FIHEP, CPHEP, DHEP, FB, and CM groups. Each group contained 5 to 17 animals. Their blood and omental lobe were obtained for blood chemistry and histopathology, respectively.

Gene Expression in Hepatocytes

The expression of albumin (Alb), cytochrome P450 (CYP), glutamine synthetase (GS), and glycerol-3-phosphate dehydrogenase (G3PDH) genes was quantified in FIHEPs and CPHEPs by real-time RT-PCR. Total RNAs were periodically extracted from them by using the RNeasy Total RNA System (Qiagen, Tokyo, Japan), 1 μg of which was used as a template to synthesize cDNAs, as reported previously [18]. The abovementioned genes were amplified using the cDNAs as templates in the PRISM 7700 Sequence Detector (Applied Biosystems Inc., Foster City, CA). Primers used were the following: Alb, CAACTACGGTGAACTGGCTGA (5′ primer) and TGCTGCAG GAAACACTCGTT (3′ primer); CYP2C7, GGCATTTTCTACTGTGT (5′ primer) and TGATAGAGGGAAGGGACTTGGAT (3′ primer); GS, CAGATGTTGGACAGGTAGCCAG (5′ primer) and CCTTAAAC TAAGCCCAGGGACA (3′ primer); G3PDH, TGCCATCACTGCCACT CAG (5′ primer) and TGCCCCACGGCCAT (3′ primer). Products under amplification were monitored directly by measuring the increase in dye intensity of SYBR Green I. The expression levels obtained were normalized against those of G3PDH.

Blood Chemistry

Sera were analyzed for concentrations of glucose (Glu), ammonia (NH_3), Alb, and total bilirubin and for glutamic pyruvic transaminase (GPT) and glutamic oxaloacetic transaminase (GOT) activity by using the FDC 3500 photometer (FUJIFILM Co. Ltd., Tokyo, Japan).

Growth Assessment of the Omental Lobe

The bromodeoxyuridine (BrdU)-labeling index was determined as follows: 1 h before sacrifice, the rats were intraperitoneally injected with BrdU at a dose of 30 mg/kg body weight and 5-fluoro-2′-deoxyuridine at a dose of 3 mg/kg body weight. After sacrifice, rat liver tissues were processed to obtain 5-μm-thick paraffin sections, and subjected to immunohistochemistry for BrdU using anti-BrdU-mouse mAbs (Dakopatts). BrdU was visualized using the Vectastain ABC Kit. The labeling index was expressed as the ratio of $BrdU^+$ hepatocytes to the total hepatocytes counted. In each liver, hepatocytes in five different photographic fields were counted.

To identify apoptotic hepatocytes, liver tissues were processed to obtain paraffin sections, and subjected to terminal deoxynucleotidyl transferase-mediated dUTP nick end-labeling (TUNEL) assay using the ApopTag Peroxidase Kit (Intergen Co., Purchase, NY). The apoptotic index was expressed as the mean ratio of $TUNEL^+$ hepatocytes to the total hepatocytes counted in five different microscopic fields for each specimen.

Characterization of Transplanted Hepatocytes

Spleen tissues were obtained from the rats 24 h post-ALF induction and were subjected to cryosectioning for immunohistochemistry and enzyme histochemistry. The cryosections were fixed in acetone at

−20°C for 5 min. Immunostaining for Alb and DPPIV was performed using rabbit anti-rat Abs (Cappel, Durham, NC) and mouse mAbs against rat DPPIV (a gift from Dr. D.C. Hixson) as the primary Ab. The Abs were visualized with the Vectastain ABC Kit (Vector Laboratories, Burlingame, CA, USA) using DAB, Texas red-conjugated goat anti-rabbit IgG, or fluorescein isothiocyanate (FITC)-conjugated goat anti-mouse IgM as a substrate. Nuclei were counterstained with hematoxylin or Hoechst 33258.

Quantification of mRNA in Hepatocyte-Transplanted Spleen

Spleen tissues were excised from the rats 24 h post-ALF induction. Total RNAs were extracted from approximately 250 mg of the tissues with the RNeasy Total RNA System, treated with RNase-free DNase I, and used for quantifying mRNAs of Alb, CYP2C7, and coagulating factor X (F-X) by RT-PCR. The primer of F-X was TGAACCTGAC CCTGAAGACCTC (5′ primer) and CAGAGGTAGTTCGGTTCGCT (3′ primer). Other primers were described previously. Similar measurements were performed for total RNAs extracted from 250 mg of liver tissues isolated from rats as a positive control.

ELISA for TNF-α, TGF-β1, IL-1β, and IL-6

Sera were collected from the rats 24 h post-ALF induction to determine the concentrations of TNF-α (Diaclone, Besançon *Cedex*, France), TGF-β1, IL-1β, and IL-6 (BioSource International, Camarillo, CA) by ELISA.

Statistical Analysis

Data are presented as mean ± standard deviation (SD). Statistical significance analysis was performed using the Kaplan-Meier survival test, log-rank test, and Student's t- test. A P value of <0.05 was considered statistically significant.

RESULTS

Propagation of Hepatocytes in Culture

As reported previously [10], hepatocytes cocultured with Swiss 3T3 cells in HCGM grew steadily and became confluent at 11 d (Fig. 1A), resulting in a 2.81 ± 0.5-fold increase in their numbers.

The levels of Alb, CYP2C7, and GS mRNAs at 1 d of culture were significantly lower than those of FIHEPs and continued to fall for up to 11 d (Fig. 1B).

Prolongation of Survival of ALF Rats by Hepatocyte Transplantation

To determine the optimal dose of hepatocytes for transplantation, the rats were transplanted with different numbers of FIHEPs (0.5, 1.0, and 1.5×10^7 cells) through the spleen. An upper limit of the injectable volume of cell suspension into the spleen was approximately 300 μL, which made the maximum injectable number of hepatocytes per animal approximately 1.5×10^7 cells. The animals were then subjected to ALF and their survival was observed (Fig. 2A). The rats that received 1.5×10^7 and 1.0×10^7 cells survived significantly longer ($P < 0.01$ and $P < 0.05$, respectively) than the control rats, which received CM alone (CM group); however, the effect of transplanting 0.5×10^7 cells was not significant. In subsequent experiments, the rats were transplanted with 1.5×10^7 FIHEPs.

We next evaluated the therapeutic potential of CPHEP transplantation in ALF. Rats were transplanted with 1.5×10^7 CPHEPs (CPHEP group) and treated for ALF, and their survival time was compared with those receiving the same numbers of FIHEPs (FIHEP group), dead FIHEPs (DHEP group), and FBs (FB group). Approximately 30% of the CPHEP group rats survived for 120 h after ALF, showing survival curves almost identical to those of the FIHEP rats (Fig. 2B). As the CM group, the FB group rats did not survive beyond 40 h, indicating hepatocyte specificity of the rescue effects of cell transplantation on liver failure. DHEP transplantation improved survival rates ($P = 0.07$ *versus* the CM group) far more than FIHEP or CPHEP transplantation. These results indicate that CPHEPs were as effective as FIHEPs in increasing the lifespan of ALF rats.

Engraftment of Hepatocytes in the Spleen

By using the DPPIV positivity of the donor HEPs, we evaluated the engraftment of the transplanted cells in the graft site (spleen) by immunohistochemical analysis. There was an abundance of DPPIV$^+$ clusters of hepatocytes at 24 h post-ALF induction in the FIHEP group, demonstrating their successful engraftment (Fig. 3A–C). These DPPIV$^+$ cells had Hoechst 33258$^+$ nuclei (Fig. 3C). Similarly, DPPIV$^+$ clusters of hepatocytes were often seen in the CPHEP-transplanted spleen (Fig. 3D). As in the FIHEP group, some of the DPPIV$^+$ cells had Hoechst 33258$^+$ nuclei (Fig. 3D–F). However, most of them lost the Hoechst 33258$^+$ nuclei (Fig. 3G–I). These Hoechst 33258$^-$ cells are considered to be dead after the engraftment in the spleen. In contrast, DPPIV$^+$ cells were absent even in the remnant liver lobe of successfully transplanted rats at any time points.

As a measure of the engraftment level of the transplanted hepatocytes, we compared the expression levels of the hepatocyte specific genes (Alb, CYP2C7, and F-X) in the spleen among the FIHEP, CPHEP, and CM groups. These levels were also compared with those of liver tissues. The expression levels in the FIHEP spleen were higher than those in the CPHEP spleen (Fig. 1C). These genes were not expressed in the CM spleen. These results support the histologic observations mentioned above, suggesting that most of the transplanted CPHEPs die soon after the engraftment. The expression levels in the FIHEP spleen were lower than those in the liver.

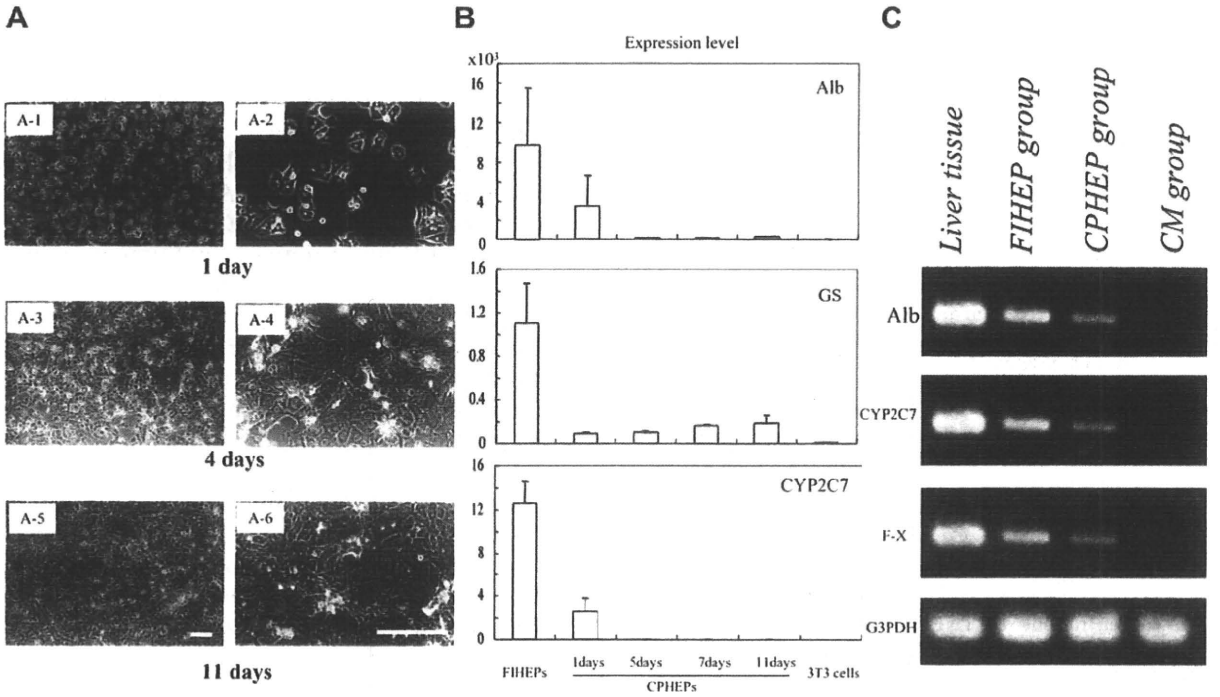

FIG. 1. (A) Phase contrast image of proliferating hepatocytes. Hepatocytes (8.5×10^3 cells/cm^2) were cocultured with Swiss 3T3 cells in HCGM on 15.0-cm dishes. Photographs were taken for the same fields at 1 (A-1, 2), 4 (A-3, 4), and 11 d (A-5, 6) with lower (A-1, 3, 5) and higher (A-2, 4, 6) magnifications. Binuclear and mononuclear hepatocytes were observed at day 1 (A-2). Hepatocytes formed clusters at 4 d (A-3) and became confluent at 11 days (A-5). Bar, 100 μm. (B) Hepatocyte marker gene expression in hepatocytes in culture. Expression of mRNAs of Alb, GS, and CYP2C7 in cultivated hepatocytes is shown. The expression levels (copy numbers) of each gene are normalized with respect to the expression levels (copy numbers) of G3PDH. (C) Hepatocyte-specific gene expression levels in the hepatocyte-transplanted spleen. The rats were transplanted with FIHEPs and CPHEPs and subjected to ALF as in Fig. 2. Control rats were given CM. Spleens were isolated at 24 h to determine the expression levels of Alb, CYP2C7, F-X, and G3PDH mRNAs by RT-PCR. Normal liver tissue was used as a positive control.

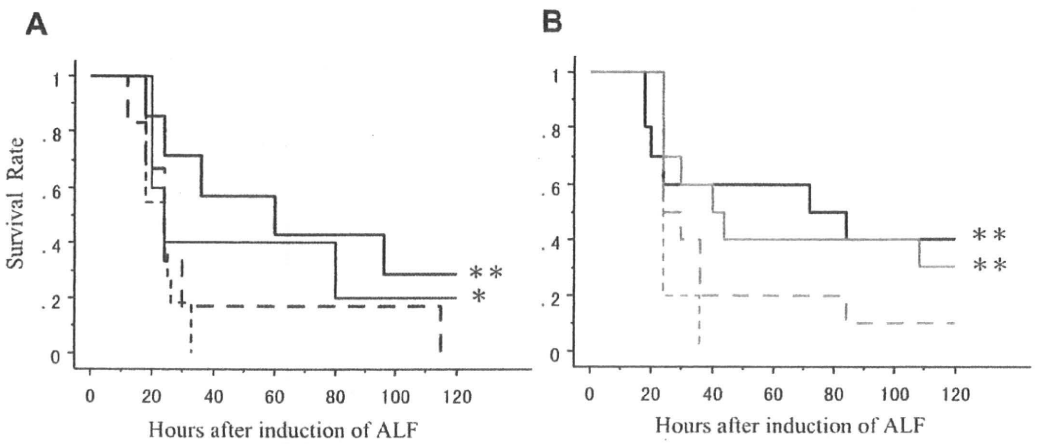

FIG. 2. Survival curves of ALF rats with FIHEP transplantation. The rats were transplanted with HEPs or FBs through the spleen and then subjected to ALF. Some rats were given CM as controls. (A) Rescue of ALF by FIHEP transplantation. The rats were given varying numbers of FIHEPs: 1.5×10^7 cells ($n = 7$, thick solid line), 1.0×10^7 cells ($n = 5$, thin solid line), 0.5×10^7 cells ($n = 6$, thick dotted line). The reference animals were given CM ($n = 11$, thin dotted line) as control. *$P < 0.05$ *versus* the CM group. **$P < 0.01$ *versus* the CM group. (B) Rescue of ALF by CPHEP transplantation. The rats were transplanted with either FIHEPs ($n = 10$, thick solid line), CPHEPs ($n = 10$, thick solid gray line), DHEPs ($n = 10$, thick gray dotted line), or FBs ($n = 5$, thin gray dotted line), 1.5×10^7 cells each, and were subjected to ALF as in (A). Some rats were given CM instead of the cells and served as controls. **$P < 0.01$ *versus* the FB group.

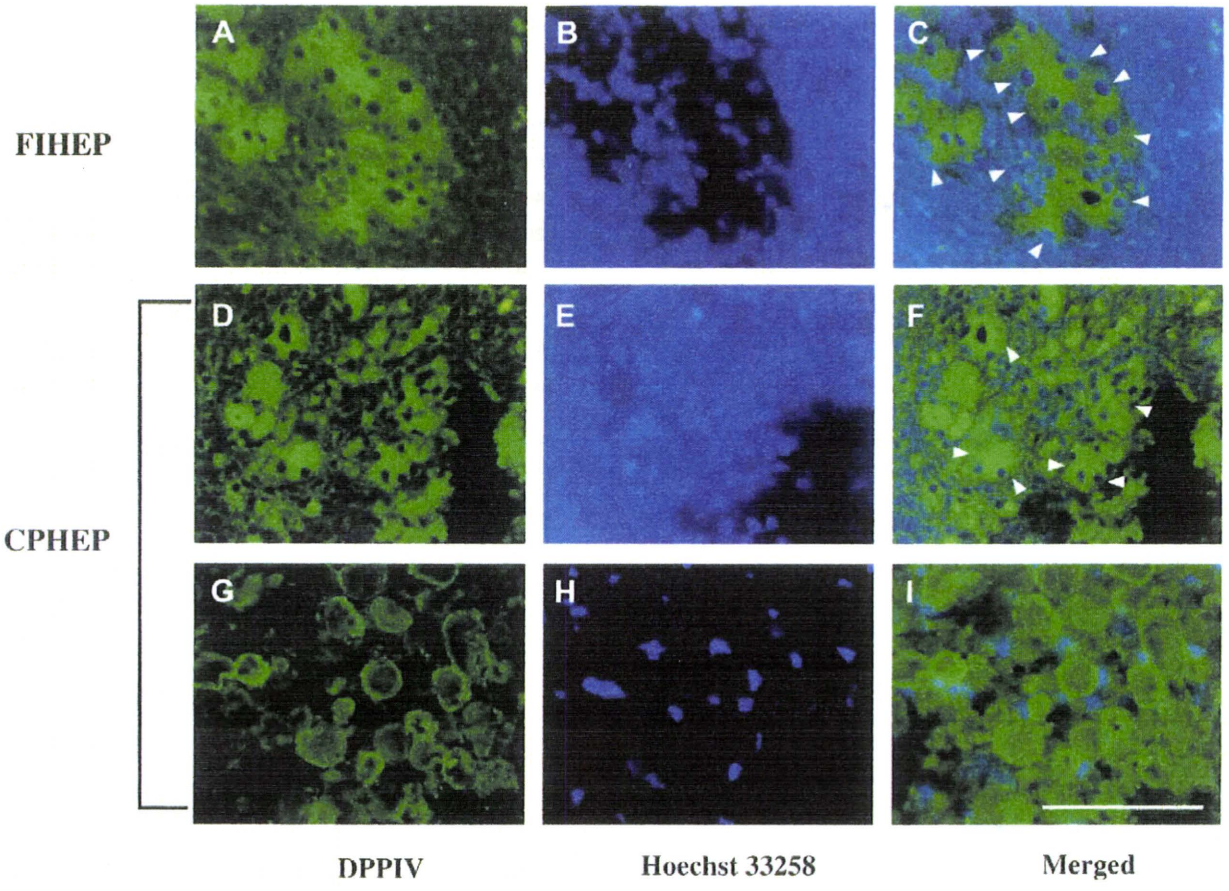

FIG. 3. Engraftment of the transplanted hepatocytes in the spleen of ALF rats. The rats were transplanted with FIHEPs (A)–(C) or CPHEPs (D)–(I) and subjected to ALF as in Figure 2B. Spleens were removed at 24 h after ALF induction and processed to cryosectioning for immunohistochemical analysis to detect DPPIV (green; A, D, G). The sections were counterstained with Hoechst 33258 [blue; (B), (E), (H)]. (A) and (B), (D) and (E), and (G) and (H) were merged into (C), (F), and (I), respectively. The arrowhead indicates $DPPIV^+$/Hoechst 33258^+ viable hepatocytes. Bar, 100 μm.

Blood Chemistry

Hepatocyte transplantation therapy for ALF was evaluated by measuring the blood levels of total bilirubin, GOT, GPT, NH_3, and Glu. The rats in the CM group showed higher levels of total bilirubin, GOT, GPT, and NH_3, and lower levels of Glu, than the hepatocyte-transplanted groups at 24 h post-ALF induction (Fig. 4), indicating that the rats experienced severe liver failure. FIHEP transplantation improved these biochemical data. The CPHEP groups showed improvement to an extent similar to the FIHEP groups. Total bilirubin and NH_3 values improved significantly, which strongly suggests that both engrafted FIHEPs and CPHEPs are functional in cholestasis and NH_3 metabolisms in ALF. However, neither FIHEP nor CPHEP transplantation significantly improved the levels of transaminase, suggesting that the transplanted hepatocytes were not sufficient to prevent ischemic changes induced by ligation of the liver lobes.

Concentrations of inflammatory cytokines in sera were also determined at 24 h post-ALF induction. TGF-β1 measured approximately 7 ng/mL, but IL-1β and IL-6 were not detected in sham-operated rats (Table 1). IL-1β and IL-6 levels in the CM group rose to approximately 300 pg/mL and 4000 pg/mL, respectively. TGF-β1 concentration in the CM group was approximately two times higher than that in sham-operated rats. IL-6 and TGF-β1 concentrations in the FIHEP and CPHEP groups became significantly lower than those in the CM group, although IL-1β concentration did not (Table 1).

Proliferation of the Remnant Liver Hepatocytes Post-ALF Induction

Hepatocyte transplantation increased the host's lifespan, suggesting that the hepatocytes in the remnant liver might be stimulated to proliferate or their cell death rates might decrease despite no gain in liver

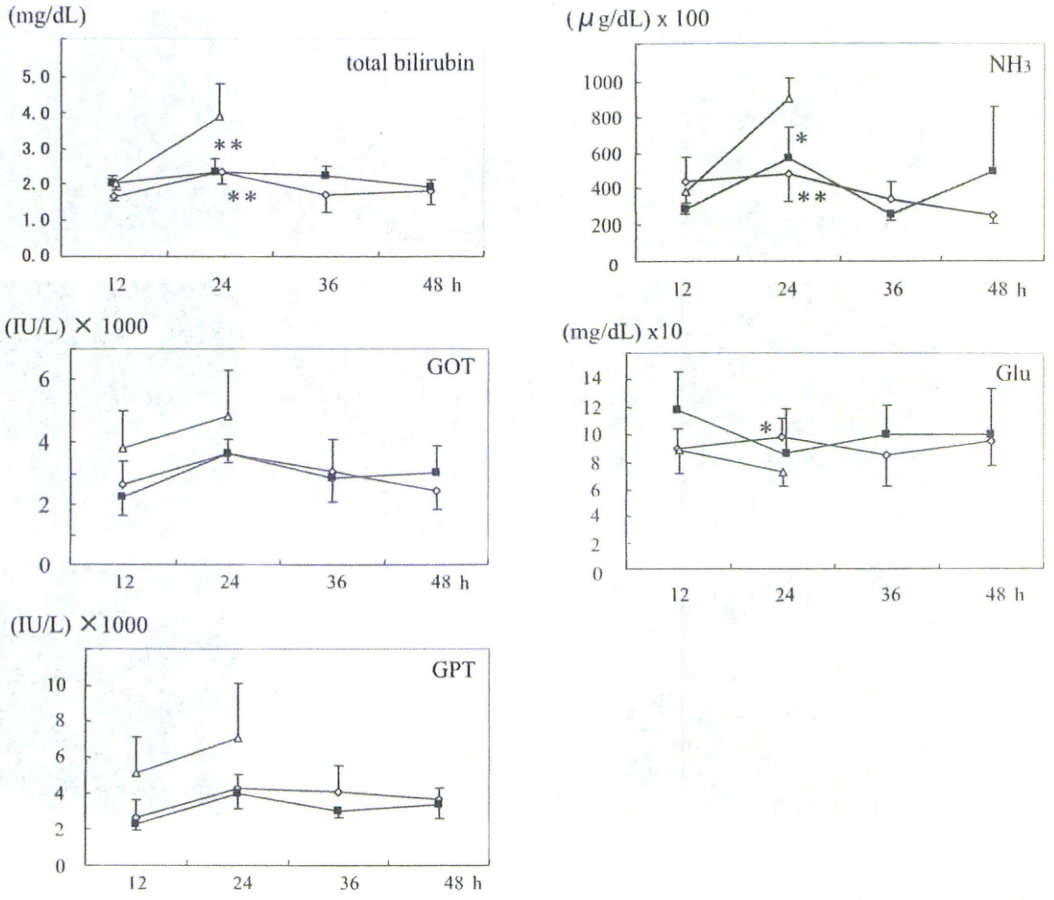

FIG. 4. Biochemical evaluation of hepatocyte transplantation therapy for ALF. The rats were subjected to hepatocyte transplantation and ALF treatment as described in Figure 2. At the indicated time points after ALF treatment, blood was collected for total bilirubin, NH_3, GOT, Glu, and GPT assessment. The mean values of total bilirubin, GOT, GPT, NH_3, and Glu in the normal control rats were 0.3 ± 0.1 (mg/dL), 75 ± 18 (IU/L), 25 ± 6 (IU/L), 151 ± 23 (μg/dL), and 197 ± 26 (mg/dL), respectively. The open diamond, closed rectangle, and open triangle indicate the FIHEP, CPHEP, and CM groups, respectively. $^{*}P < 0.05$ *versus* the CM group. $^{**}P < 0.01$ *versus* the CM group.

weight within the experimental period (up to 5 d). To address this possibility, the BrdU-labeling index and TUNEL activity were determined as a measure of cell proliferation activity and cell death, respectively. BrdU-labeling indexes at 24 h post-ALF in the CM, FIHEP, and CPHEP groups are shown in Figure 5A-1, A-2, and A-3, respectively. $BrdU^+$ nuclei were present in the FIHEP and CPHEP groups but were scarce in the CM group. These $BrdU^+$ hepatocytes were host hepatocytes because they were $DPPIV^-$. The BrdU-labeling indexes are shown in Figure 5A-4. The indexes at 12 h were low (<2%) and not significantly different among the three groups of rats. The indexes of the FIHEP and CPHEP groups at 24 h significantly increased, compared with those of the CM group. At 48 h post-ALF, there was a similarly large increase in the labeling indexes (>10%) in both the FIHEP and CPHEP rat livers, indicating that CPHEP transplantation stimulated the proliferation of the remnant hepatocytes as effectively as FIHEP transplantation. In a parallel experiment, some sections at 24 h post-ALF were stained for TUNEL activity. $TUNEL^+$ hepatocytes were frequently observed in the CM rats (Fig. 5B-1) but decreased substantially in the FIHEP (Fig. 5B-2) and CPHEP (Fig. 5B-3) rats. The ratios of the $TUNEL^+$ hepatocytes to the total hepatocytes are shown in Figure 5B-4 as apoptotic indexes. The apoptotic index

TABLE 1

Comparison of Inflammatory Cytokines 24 h Post-ALF Induction

Exp. group	IL-1β (pg/mL)	IL-6 (pg/mL)	TGF-β1 (ng/mL)
SO	ND	ND	7.27 ± 3.16
FIHEP	382.1 ±107.3	499.8 ± 485.6	10.56 ± 4.21*
CPHEP	418.1 ± 73.8	337.4 ± 150.7*	10.79 ± 1.94*
CM	329.1 ± 32.8	4375.5 ± 5568.9	15.27 ± 2.74

ALF = acute liver failure; SO = sham operation; ND = not detected. FIHEP = freshly isolated hepatocyte; CPHEP = culture-propagated hepatocyte; CM = culture medium

Sham operation indicates laparotomy alone.

$^{*}P < 0.05$ *versus* the CM group.

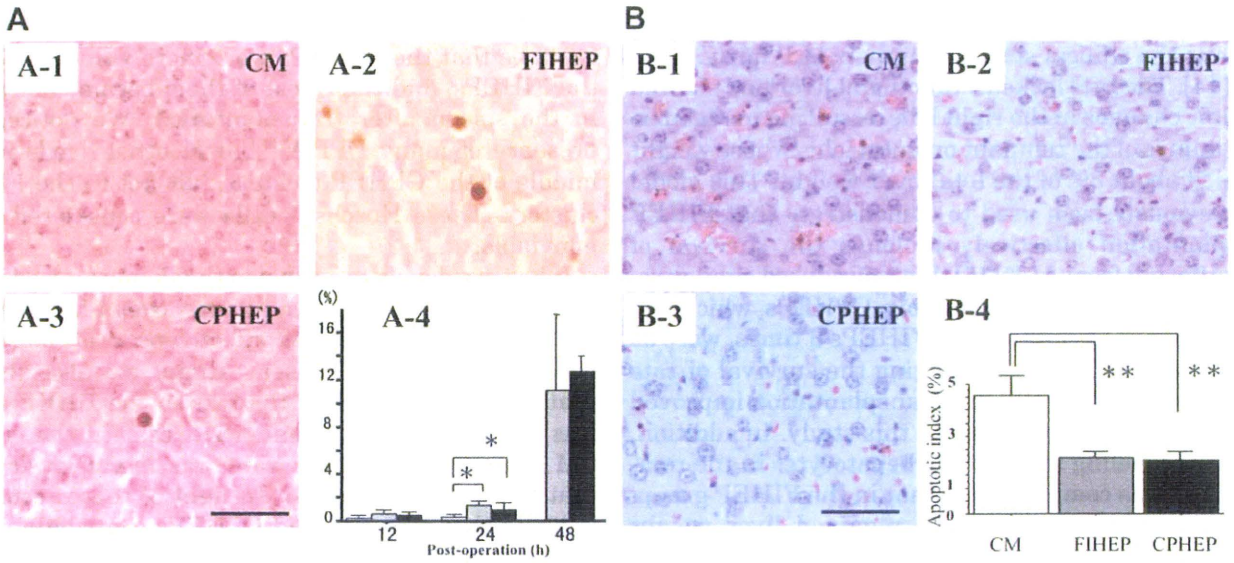

FIG. 5. (A) BrdU-labeling index of hepatocytes in the remnant liver of the hepatocyte- transplanted rat. The rats were injected with CM, transplanted with FIHEPs or CPHEPs, and subjected to ALF as in Fig. 2. The remnant livers (omental lobe) were removed at 12, 24, and 48 h post-induction of ALF and processed to obtain paraffin sections for BrdU staining. (A-1), (A-2), and (A-3) are representative of photos from rats with CM, FIHEPs, and CPHEPs, respectively, taken at 24 h post-ALF. $BrdU^+$ nuclei are brown in color. In (A-4), $BrdU^+$ cells were counted from five microscopic fields of each section from 4 rats in each group at the time points indicated, and the BrdU-labeling index was calculated as the ratio of $BrdU^+$ cells to the total cells in a counted field. The open bar, gray bar, and black bar indicate the CM, FIHEP, and CPHEP groups, respectively. $*P < 0.05$ *versus* the CM group. Bar, 50 μm. (B) Suppression of remnant hepatocyte apoptosis by hepatocyte transplantation. The rats were transplanted with hepatocytes and subjected to ALF as described in Fig. 2. Paraffin sections were prepared from the remnant livers (omental lobes) isolated from the CM (B-1), FIHEP (B-2), and CPHEP groups (B-3) at 24 h post-ALF and were stained for TUNEL activity. $TUNEL^+$ pycnotic nuclei (brown) were frequently observed in the CM group, but less often in the FIHEP and CPHEP groups. Apoptotic cells were counted from five microscopic fields of liver tissue sections from four rats in each group. The ratio of apoptotic cells to total cells in the counted field was expressed as the apoptotic index (B-4). The open bar, gray bar, and black bar indicate the CM, FIHEP, and CPHEP groups, respectively. $**P < 0.01$ *versus* the CM group. Bar, 50 μm.

of the remnant liver in the FIHEP and CPHEP groups decreased to approximately 50% of that in the CM group. These $TUNEL^+$ hepatocytes were host hepatocytes because they were $DPPIV^-$. Thus, CPHEP transplantation suppressed the apoptotic changes in the host hepatocytes as effectively as FIHEP transplantation.

DISCUSSION

Although several studies have supported the effectiveness of hepatocyte transplantation in treating patients with ALF, there is a severe problem in using hepatocyte transplantation therapy as a general clinical treatment for patients with liver failure: owing to the lack of donor organs available for clinical use, hospitals cannot supply sufficient quantities of normal human hepatocytes to such patients. One way to overcome this limitation might be to devise a method of abundantly propagating hepatocytes in culture, starting with a small amount of hepatocytes isolated from small pieces of available liver tissues. However, it does not seem to be a practical solution, because it is well documented that normal hepatocytes show poor multiplication ability *in vitro* despite their remarkable growth potential *in vivo* [19].

We have been engaged in developing a technology to abundantly propagate hepatocytes in culture [8, 9] and previously reported that rat hepatocytes were capable of repeatedly multiplying *in vitro* when cocultured with Swiss 3T3 cells in a medium that we devised [10]. We have now shown that such CPHEPs can be used as a source of hepatocyte transplantation for preventing hepatectomy-induced ALF. Resection of hepatic tumors is currently the gold standard treatment for patients with either primary or secondary liver malignancies. An extended hepatectomy is often necessary to achieve curative resection; however, ALF after massive hepatectomy remains a challenging problem (i.e., the risk of insufficiency of remnant liver volume, leading to unresectability). If we devise a countermeasure to prevent ALF beforehand, aggressive hepatic resection could be safely performed. Seeking to answer this clinical question, we evaluated the prevention efficacy of CPHEP transplantation in a surgical model of hepatectomy-induced ALF.

To estimate the efficacy of transplanting either FIHEPs or CPHEPs in ALF, we employed an experimental ALF model induced by subjecting rats to two-thirds-hepatectomy and ligation of the right-lobe pedicle. This method induces more severe liver failure than

a model induced by 90% hepatectomy and is considered to mimic the clinical status of human ALF fairly faithfully [14]. The rats lacked a functional liver and showed ischemic changes in the right lobe, resulting in regeneration failure of the remnant omental lobe, whose weight occupied about 8% of the total liver weight. This model has previously been used to demonstrate that FIHEP transplantation effectively prolongs the survival of rats suffering from ALF [15]. We reproduced similar results in the present study. Notably, CPHEPs, which had been prepared by multiplying FIHEPs 3 times, were as effective as FIHEPs in prolonging the survival of rats suffering from ALF. CPHEP transplantation improved all the liver functions tested in this study. In addition, the BrdU-labeling index of the hepatocytes in the remnant liver was comparable to that in the FIHEP group. Rats with CPHEPs gradually regained liver weight after ALF induction, as did those with FIHEPs. These results together indicate that both CPHEP and FIHEP could be a source for hepatocyte transplantation to promote regeneration of the remnant liver after ALF induction.

There have been two explanations for lethal hepatic failure after excessive hepatectomy: hepatectomy causes microcircular disturbances [20] or induces cytotoxic factors such as TNF-α, TGF-β1, and oxidative stress-related factors [21, 22]. In the present study, we did not find any evidence of microvascular disturbances on hematoxylin and eosin (H&E)-stained sections of the remnant lobe in the ALF-induced rats, but we did observe hypercytokinemia of cytokines such as IL-6 and TGF-β1. Apoptotic hepatocytes were frequently seen by TUNEL assay in the remnant liver lobe of the ALF-induced rats. CPHEP and FIHEP transplantation decreased the concentrations of IL-6 and TGF-β1 in sera, as well as the frequency of apoptotic hepatocytes. Therefore, it appears that both CPHEPs and FIHEPs prolonged the survival of ALF-induced rats by suppressing the hepatocytic apoptosis in the remnant liver.

In the present study, we demonstrated the presence of $DPPIV^+$ hepatocytes in the spleen at 24 h after ALF induction, which clearly indicated the engraftment of both transplanted CPHEPs and FIHEPs in the graft site. There were no significant differences in the frequency of $DPPIV^+$ hepatocytes between the FIHEP and CPHEP groups. However, the expression level of hepatocyte-specific mRNAs such as Alb, CYP2C7, and GS in the spleen of the CPHEP rats was considerably lower than that in the FIHEP rats. This might be explained by the fact that CPHEPs showed lower expression levels of these marker genes than FIHEPs at the time of transplantation; this was due to the fact that the CPHEP cells had been cultured for 11 d before transplantation, during which time the expression levels had decreased (Fig. 1B). Another explanation could be that the CPHEPs were more vulnerable than the FIHEPs, and that most of them became nonviable in the spleen after transplantation. We noticed the presence of many $DPPIV^+$ but $Hoechst^-$ cells in the middle of the CPHEP clusters, but not in the FIHEP clusters. These $Hoechst^-$ cells were considered to be nonviable.

It has previously been shown that homogenized hepatocytes were even effective as a treatment for liver failure [23], suggesting the effectiveness of nonviable hepatocytes. In the present study, we also showed that the survival rate of the rats in the DHEP group was better, to some extent, than that in the control CM group, although the rate was much lower than that of the CPHEP group. In light of these results, it is likely that transplanted CPHEPs contribute to the improvement of liver failure by substituting the function of the host liver. They may also provide some growth factors or enzymes to support the regeneration of the remnant liver. It remained to be elucidated whether the cryopreserved CPHEPs also display such beneficial effects. Hepatocytes are known to be very sensitive to freezing damage. Three distinct modes of cryopreservation-induced hepatocyte death have been identified, namely, physical cell rupture, necrosis, and apoptosis [24]. The susceptibility of hepatocytes to such freeze-thaw injury is attributed to the damage to mitochondria, including loss of mitochondrial membrane integrity, increase in membrane permeability, etc. The inhibition of mitochondria damage, for instance, by broad-spectrum caspase-inhibitor, would prevent cryopreservation-induced damage of propagated hepatocytes.

In conclusion, the transplantation of homologous CPHEPs has a remarkable therapeutic potential for ALF in rats. Since we have recently established a culture method that enables us to multiply human hepatocytes 50 to 100 times during 50 d of culture [25], CPHEPs might be a useful source of hepatocytes for transplantation to treat human patients with ALF.

REFERENCES

1. Lee WM. Acute liver failure. N Engl J Med 1993;329:1862.
2. Bismuth H, Samuel D, Casting D, et al. Orthotopic liver transplantation in fulminant and subfulminant hepatitis. Ann Surg 1995;222:109.
3. Moreno GE, Garcia GI, Loinaz SC, et al. Liver transplantation in patients with fulminant hepatic failure. Br J Surg 1995;82:118.
4. Gewartowska M, Olszewski WL. Hepatocyte transplantation-biology and application. Ann Transplant 2007;12:27.
5. Habibullah MC, Syde HI, Qamar A, et al. Human fetal hepatocyte transplantation in patients with fulminant hepatic failure. Transplantation 1994;58:951.
6. Strom SC, Fisher RA, Thompson MT, et al. Hepatocyte transplantation as a bridge to orthotopic liver transplantation in terminal liver failure. Transplantation 1997;63:559.